



**Politecnico
di Torino**

Politecnico di Torino

Master of Science in Environmental and Land Engineering – Climate Change

A.a. 2021/2022

Graduation session October 2022

Master Thesis

**Impacts of climate change on maize
irrigation in the North-west of Italy and
possible adaptation strategies**

Supervisor:

Prof. Stefania Tamea

Candidate:

Giulia Pezzin

Co-supervisor:

Dr. Matteo Rolle

Abstract

FAO estimates that by 2050 agriculture will have to increase its production worldwide by almost 50% compared to 2012 to be able to satisfy the global demand for food, livestock fodder and biofuels. Climate change brings urgency and uncertainty to this problem. It is fundamental to implement effective adaptation strategies for agricultural practices but, to do so, regional and local studies about the potential impacts of climate change are needed. In this work, a local impact study is performed on an area located in the north-west of Italy, which already suffers from irrigation water supply problems. The final objective is to obtain useful estimates for the future implementation of adaptation strategies. To reach this objective, a daily-scale hydrological crop model is used to compute temporal series of daily actual evapotranspiration and daily irrigation requirements from 2006 to 2055, considering two future climate scenarios (RCP2.6 and RCP8.5). The crop analyzed is maize since it is the most present crop in the area in terms of fraction of irrigated utilized agricultural area. The results show that summer is the critical season for maize development because if not irrigated, it suffers from water stress from June to September. This means that, at the study site, maize must be irrigated to secure a proper production. In the future, there is a wide range of possibilities depending on the future climate scenario examined. Considering RCP2.6 scenario, the irrigation requirements are projected to decrease from 2006 to 2050. On the contrary, under RCP8.5 hypothesis the irrigation requirements will increase in the future compared to the present values, mainly due to the reduction of total summer precipitations and the rise of summer temperatures. However, the inter-annual variability of the results from both the climate scenarios is high. Two adaptation strategies are analyzed, trying to reduce the projected irrigation requirements. The early sowing of maize demonstrates to be a possible effective strategy, since it allows a decrease of the water needs in every case, with peaks of over 20% of reduction. On the other hand, the second adaptation strategy, substituting maize with alternative crops, does not give the expected benefits. Wheat and potatoes were chosen as possible alternatives because they are both already cultivated at the study site, and they have a similar crop calendar to maize. However, the projected irrigation requirements for these two crops results to be higher than maize's.

Contents

Abstract.....	2
Introduction	5
Chapter 1 Crop model.....	8
<i>1.1 Evapotranspiration.....</i>	<i>8</i>
<i>1.2 State of the art of crop models.....</i>	<i>9</i>
<i>1.3 Crop model features</i>	<i>10</i>
1.3.1 Model's input data	11
1.3.2 Model's outputs	13
Chapter 2 : Climate data.....	15
<i>2.1 Observations.....</i>	<i>15</i>
<i>2.2 Climate projections for RCP2.6 and RCP8.5 scenarios.....</i>	<i>16</i>
2.2.1 Climate scenarios.....	16
2.2.2 Climate models	17
Chapter 3 Case study and preliminary analyses	21
<i>3.1 The area of interest.....</i>	<i>21</i>
3.1.1 Selection of temporal series	25
<i>3.2 Validation.....</i>	<i>27</i>
3.2.1 Minimum and maximum temperature	28
3.2.2 Precipitations	29
<i>3.3 Bias Correction</i>	<i>30</i>
<i>3.4 Variables trends analysis</i>	<i>31</i>
3.4.1 Precipitations	32
3.4.2 Temperature.....	34
<i>3.5 Reference evapotranspiration</i>	<i>35</i>
Chapter 4 Crop model results	38
<i>4.1 Present results</i>	<i>38</i>

4.2 <i>Future projections</i>	41
4.2.1 Crop water requirements and actual evapotranspiration	41
4.2.2 Water stress	43
4.2.3 Irrigation requirements	46
4.3 <i>Crop adaptation, early sowing</i>	50
4.3.1 Crop water requirements and water stress	51
4.3.2 Irrigation requirements	55
4.4 <i>Crop adaptation, alternative crops</i>	57
Chapter 5 Conclusions	60
References	63
Appendix I – Climate projections databases	67
Appendix II – Validation graphs for T_{max} and T_{min}	69
Appendix III – Validation graphs for precipitations	72
Acknowledgments	75

Introduction

Climate change has become one of the main points of discussion both from the general public and from the scientific community, and nowadays it is gaining attention also from the policy makers. Climate change is already affecting countries all around the globe and its impacts have been well documented. The global temperature has increased since 1850 and there is evidence of change in climate extremes, such as heatwaves and droughts, in every region across the globe (IPCC, 2021).

These changes affect, between all the other things, also one of the crucial economic activities for the development of human society: agriculture. Agriculture is strategic on the global level, generating as an economic sector between 1% and 60% of national GDP in many countries of the world, with a world average of about 4% (Mbow, 2019). Its economic importance reflects its fundamental role in the survival of the human population, with its main expression being the production of food. The problem of feeding all the human population is indeed one of the biggest problems of the millennium (FAO, 2021b), the solution of which has its core in agriculture development. In the report *The state of the world's land and water resources for food and agriculture: Systems at breaking point* (FAO, 2021b), it is stated that:

“By 2050, FAO estimates agriculture will need to produce almost 50 percent more food, livestock fodder and biofuel than in 2012 to satisfy global demand and keep on track to achieve “zero hunger” by 2030”.

However, the challenges to achieve this goal are several. An agricultural production of such a magnitude comes with some downsides, i.e. it generates pressures on land, soil, and water resources. Today, those pressures are at such a critical point that it is compromising the agricultural productivity in itself (FAO, 2021b). For example, the over 30% increase in food supply per capita from the 1960s has been accompanied by an increase of more than 100% of the water used for irrigation (Mbow, 2019). Nowadays, agriculture accounts globally for the 72% of all surface and groundwater withdrawals (FAO, 2021b) and these withdrawals are bringing many water systems to the breaking point. So, the challenge for agriculture is to keep sustaining the production levels while reducing land degradation and emissions together with preventing further loss of environmental services.

Climate change brings uncertainty and urgency to this challenge, with changing precipitations and drought patterns, warmer mean and extreme temperatures etc. affecting the food production worldwide.

Given this, it is fundamental to talk about adaptation strategies for agricultural practices to mitigate the impacts of climate change on the sector and secure food production. With adaptation strategies it is meant all the responses to actual or projected climate change effects that moderate its harms and exploit its beneficial opportunities. Some examples of adaptation strategies for agriculture are:

- Planting of drought resistant varieties of crops;
- crop diversification;
- change in cropping pattern and calendar of planting;
- improve irrigation efficiency.

In order to implement effective policies to adapt the agricultural practices, regional and local studies of climate change potential impacts are needed.

This study is indeed an impact study focused on a small area in the north-west of Italy, part of the region of Piedmont. This region too was affected by the exceptional drought that happened in Italy in early 2022, which caused a reduction of 60% of the precipitations over the national territory compared to the historical mean for the same period (Cappellini, 2022). This drought provided an example of the vulnerability of the national agricultural system. Because of the water shortage indeed, in Piedmont the damages to agriculture were huge, with for example a reduction of maize production that reached in some areas the 50% (IlPuntoColdiretti, 2022). In Piedmont region, trends in historical series of observations over the last 60 years (1958-2018) already show a reduction of 13% of the winter precipitations and an increment of the daily maximum temperatures of 2°C (Arpa Piemonte, 2020b), so it seems safe to assume that extreme events like this recent drought will happen again in the future. Furthermore, the agricultural sector in Piedmont is important, with 36% of the territory dedicated to agricultural production (IRES Piemonte, 2019), which in this region is strongly based on irrigation with 55% of the utilized agricultural area of the local districts considered being irrigated (ISTAT, 2010). Given these considerations, implementing strategies to face climate change impacts on the sector and improve the production under these new climatic conditions seem fundamental for Piedmont.

The present study places itself in this context, aiming at assessing the local impacts of climate change on the water needs of crops (in particular, maize) at a local level, to see how much it could change in the future (in two different climate scenarios, RCP2.6 and RCP8.5). The final objective is to obtain useful data and information for the future development and implementation of adaptation strategies of agriculture in the studied local area.

In particular, this work analyzes the changes of irrigation requirements and actual evapotranspiration of maize, one of the most common crops of the area, over the period 2006-2055. To do so, an existing crop model (Rolle et al, 2021) has been adapted and applied to the local scale of interest.

Chapter 1 Crop model

1.1 Evapotranspiration

Evapotranspiration and soil water balance are the core of this study, so some concepts and definitions will be presented here to provide a useful basis to start the more detailed discussion on.

Evapotranspiration is defined by FAO, the Food and Agriculture Organization of the United Nations, as “the combination of two separate processes whereby water is lost on the one hand from the soil surface by evaporation and on the other hand from the crop by transpiration” (Allen et al., 1998). The need of referring to evaporation and transpiration as the single phenomenon of evapotranspiration (ET) instead of two separate ones comes from the fact that these two phenomena happen at the same time, and it is very difficult to distinguish between them. The ET rate expresses the amount of water lost from a cropped surface in units of water depth, and its unit of measure is normally millimeters (mm) per unit time (Allen et al., 1998).

According to FAO’s guidelines, there are three types of evapotranspiration (Allen et al., 1998):

- *Reference evapotranspiration ET_0* : the evapotranspiration rate from a reference surface, i.e., a hypothetical grass reference crop with specific characteristics (height of 0.12 m and albedo equal to 0.23). ET_0 depends only on climate parameters.
- *Crop evapotranspiration ET_c* : the evapotranspiration rate from a crop in standard (optimal) conditions, i.e., disease-free, well-fertilized, under optimum soil water conditions, which then achieves full production under the given climatic conditions. It is calculated considering a crop coefficient k_c to take into account the specific crop characteristics:

$$ET_c = k_c \cdot ET_0 \tag{1.1}$$

- *Actual evapotranspiration ET_a* : the evapotranspiration from crops grown under management and environmental conditions that differ from the standard conditions (non-optimal conditions). It then depends not only on the weather and crop characteristics, but also on the specific field conditions and agricultural practices. The

water stress coefficient k_s is introduced to represent the effects of water insufficiency on plants development:

$$ET_a = k_s \cdot ET_c \quad (1.2)$$

k_c [-] for a given crop changes from sowing till harvest because of the variations in the crop characteristics throughout its growing season (initial stage, growth, mid-season, senescence). k_s [-] varies from 0 to 1 and depends on the water content of the soil. k_s equal to 1 means that there is no water stress (available water is sufficient for the plant), while k_s equal to 0 corresponds to the wilting point (the plants cannot grow properly).

1.2 State of the art of crop models

In the recent years, there have been several studies that used gridded crop models to estimate irrigation requirements of food production on a global level, as well as some that focused on regional scale (continental or national scale). A useful and comprehensive work of intercomparison between multiple global gridded crop models (GGCMs) has been performed in the framework of AgMIP (Agricultural Model Intercomparison and Improvement Project) and ISIMIP (Inter-Sectoral Impacts Model Intercomparison Project) (Rosenzweig et al., 2014). It tested seven GGCMs driven by five global climate models, focusing mainly on yield, with the aim of characterizing the uncertainty cascade for this type of simulations.

There are many important projects on the global scale, but recently also a drive for improving the spatial resolution of crop water requirements has risen, because impact studies and adaptation strategies need results and information on finer scales (often, local scales). The spatial resolution of global crop models has indeed improved over the years, also thanks to new crop-specific datasets of irrigated areas (Rolle et al., 2021). Nonetheless, the majority of previous crop models still provided results with a spatial resolution too coarse for local impact studies and they were rarely based on daily data (Rolle et al., 2021).

This study fits in this context, with the aim of assessing future impacts of climate change on the crop water use (in particular, irrigation requirements) at a local scale and with daily timeseries, adapting a hydrological crop model previously used for global assessments to a smaller area of study.

1.3 Crop model features

The crop model used in this study is an existing daily-scale hydrological model developed by Rolle et al. (2021), operating in both rainfed and irrigated scenarios. The main model's outputs are irrigation requirements (irrigated scenario) and actual evapotranspiration (rainfed scenario), calculated using a soil-water balance approach with the input of climatic data and agricultural information (Rolle et al., 2021). The focus of this work is to study the temporal variability of the situation in details, so the model was used on a single cell, leaving out the study of the spatial variability.

The model calculates the actual evapotranspiration ET_a for each i -day of the year according to FAO's approach (Allen et al., 1998), with the equation:

$$ET_{a,i} = ET_{0,i} \cdot k_{c,i} \cdot k_{s,i} \quad (1.3)$$

where $ET_{a,i}$ and $ET_{0,i}$ are respectively the actual and reference evapotranspiration for the i -day in mm/day, $k_{c,i}$ is a dimensionless coefficient called the crop coefficient, and $k_{s,i}$ is the water stress coefficient (between 0, wilting point, and 1, no water stress).

To calculate the expression above, the model mimics a soil-water balance for each i -day of the year with a step procedure:

1. It calculates the daily crop coefficient, k_c , depending on the crop chosen and the period of the growing season.
2. From the daily precipitations, it obtains the increment of Soil Moisture.
3. Two variables are then computed, the daily maximum water capacity in the rooting zone (TAW) and the amount of water available until water stress occurs (RAW).
4. It calculates the water stress coefficient k_s , on which the minimum amount of irrigation requirement for the i -day depends. If k_s is kept at 1, the model will consider the water needed to reach field capacity, while considering $k_s < 1$ allows to analyze deficit irrigation strategies.
5. At this point the model can calculate the actual evapotranspiration ET_a for the i -day.
6. The reduction of the soil moisture due to the daily ET_a (deficit increase) is computed.
7. The *final soil moisture* at the end of the day is calculated, which will be used as *initial soil moisture* for the balance of the following day.

These are the steps which result in the daily ET_a timeseries in rainfed conditions. In the case of irrigation, two additional steps are added between step 6 and 7 that allows to calculate the daily timeseries of ET_{green} (i.e., the part of ET_a satisfied by precipitations), and irrigation requirements $IrrReq$. For a detailed description of all the variables and data needed for this procedure and its outputs, see the next sections (1.3.1 and 1.3.2).

1.3.1 Model's input data

In the following paragraphs all the inputs needed to run the model as a Matlab function are briefly introduced and some main set up choices for the runs are explained. More in-depth description of the climatic datasets used is provided in Chapter 2.

Crop type

The model is designed for 26 different crops, both perennial and temporary. Maize, number 2 of the list, was selected because it is the main cultivation of the agricultural season of 2009-2010 in the area studied (ISTAT, 2010). In Chapter 3 the characteristic of the considered area will be discussed in detail.

Climatic region

Another choice to make is between the ten climatic regions of the world for which the model has been designed (Rolle et al, 2022). Those regions are defined according to the agroecological classification proposed by FAO (FAO, 2021a) and they are the following: Tropical, Sub-Tropical (summer rainfall), Sub-Tropical (winter rainfall), Oceanic Temperate, Sub-Continental Temperate, Continental Temperate, Boreal Oceanic, Boreal Sub-Continental, Boreal Continental, Arctic. The characteristics of the crop-specific growing phases change depending on the climatic region in which the crop grows. For this work the climatic region set for all the runs as the one that better represents the climatic characteristics of the studied area is Sub-Continental Temperate (number 5).

Growing season

Regarding temporary crops, the model also asks for two parameters describing the growing season: the sowing and harvesting dates. The dates need to be in the form of number of days

since the start of the year, i.e., 1 is the 1st of January while 365 is the 31st of December. Sowing date and harvesting date were set as the 16th day of the sowing month and 15th day of the harvesting month, in agreement with previous literature (Tuninetti et al., 2015). This assumption was necessary because the database used for sowing and harvesting days, MIRCA2000, gives info only on a monthly basis. MIRCA2000 is a crop-specific and global database of monthly growing seasons, with a spatial resolution of 0.0833° (Portmann et al., 2010). Given all the previous considerations, the two dates set for all the model runs were the days number 106 and 258, which represent the 16th of April (sowing date) and the 15th of September (harvesting date) respectively.

Initial soil moisture

The model computes the outputs through a soil-water balance, so information about soil moisture (SM) is necessary. Specifically, there are two inputs of the model function related to SM: *initial soil moisture* and *sowing soil moisture*. The *initial soil moisture* (m^3 of water/ m^3 of soil) is the soil moisture at the beginning of the i -day, before the soil water balance of that day. For temporary crops, this number is the one computed by the model for the day before (saved as *final_SM* of the $(i-1)$ -day by the model). *Sowing soil moisture* (m^3 of water/ m^3 of soil) instead is the soil moisture on the sowing date. Mean monthly values of daily SM for the period 1970-2019 were used to set a reasonable value for the sowing soil moisture, i.e., the mean value for April (0.2 m^3 of water/ m^3 of soil) was given as input to the model. This value is the same as the set *AWC* value (see next paragraph), so it is like assuming the soil moisture on the sowing day equals field capacity. This is coherent with previous studies performed with this model which assumed the same thing (Rolle et al., 2022).

Available water capacity (AWC)

The *available water capacity* (m^3 of water/ m^3 of soil) is the water in the soil readily available to plants, assumed to be the difference between the water content at field capacity (the maximum amount of water that the soil can store after drainage) and water content at wilting point (minimum amount of water needed by the crop, with less water than wilting point the plants stop evapotranspiration). For this study, *AWC* has been set at 0.2 m^3 of water/ m^3 of soil, a value obtained after the elaboration of data from global SoilGrids dataset according with the procedure described by Rolle et al. (2022).

Precipitation and reference evapotranspiration (ET_0)

Precipitation and ET_0 are the two inputs that represents the climate variability in the model. The format required by the function for these two data is a matrix for each variable with daily values expressed in mm/day. Daily values for precipitation (P), maximum temperature (T_{max}) and minimum temperature (T_{min}) have been retrieved from future projections by an ensemble of climate models for two different climate scenarios (RCP.2.6 and RCP8.5), covering the time period 2006-2055. ET_0 was then computed from T_{max} and T_{min} following the Hargreaves-Samani method. For more details on climatic data analysis and ET_0 computation see Chapter 2 and Chapter 3.

1.3.2 Model's outputs

The results from the model computations are arranged in matrices of the same dimensions of the inputs P and ET_0 . Specifically, they are daily timeseries for the years modeled. The following variables are the main outputs of the model and those useful for the discussion of the results of this study.

Water stress coefficient k_s (-)

k_s is the coefficient that represents the stress caused to the plant by water deficit, and so the consequent decrease of production. The model computes daily timeseries of this coefficient as an intermediate step of its process, but there is the useful possibility of saving its timeseries too. In particular, k_s timeseries will be analyzed for rainfed scenario, to better understand the situation in case of water deficit.

Actual evapotranspiration (mm)

Actual evapotranspiration ET_a considers the effects of water stress on the crop. It is obtained by multiplying the crop evapotranspiration by the water stress coefficient k_s . It is the main output of the model in rainfed conditions.

Crop evapotranspiration (mm)

The crop evapotranspiration ET_c is not a direct output of the model, but something it calculates as an intermediate step of the calculation. Since it is useful to consider it to have a meter of comparison for ET_a and to compute the crop water requirement (CWR), daily series of ET_c were calculated subdividing daily ET_a by daily k_s series.

Green Evapotranspiration (mm)

The green evapotranspiration (ET_{green}) is the part of actual evapotranspiration that is supplied by precipitations (i.e., soil moisture due to precipitations). The actual evapotranspiration can be subdivided into two components, ET_{green} and ET_{blue} , as shown by the following expression:

$$ET_a = ET_{green} + ET_{blue} \quad (1.4)$$

ET_{blue} represents the water used by the plants coming from surface water bodies, groundwaters, and reservoirs. It is usually provided by irrigation, when precipitations are not sufficient to fulfill the water needs of the crop.

Irrigation requirements (mm)

The irrigation requirement ($IrrReq$) represents the minimum water depth needed by the crop to avoid water stress, when precipitations are not sufficient, consistently with the definition given in Rolle et al. (Rolle et al., 2021). It is a step further from ET_{blue} , since it considers for the sowing day the sum of two irrigation components: evapotranspirative component (ET_{blue}) and water for soil component (i.e., the additional water required to bring soil moisture at the specific defined level on the sowing day). $IrrReq$ is a theoretical estimation of the water that would be needed to have the maximum efficiency of production, it does not represent the actual water volume that would be (or will be) supplied to the plants since this quantity would depend also on the irrigation systems used and their efficiency, as well as other factors independent from the simulation performed in this study (limits to the water available for irrigation because of droughts etc.).

Chapter 2 : Climate data

As introduced in Chapter 1, the crop model requires various input data. Specifically, precipitation (P) and reference evapotranspiration (ET_0) are the input data related to climate. To calculate ET_0 , maximum and minimum daily temperature were used. Given that, the climate data needed for the study were daily precipitation P , daily maximum temperature T_{max} , and daily minimum temperature T_{min} .

Two types of climate data were used in this study:

- Observations;
- climate projections (RCP2.6 and RCP8.5 scenarios).

2.1 Observations

Observations of daily precipitation, daily maximum temperature and daily minimum temperature were taken from the ARPA Piemonte dataset called NWIOI (Arpa Piemonte, 2017). These data were used to validate the models' results for the period 2006-2020. NWIOI consists in those three daily variables distributed on a regular grid over Piemonte region. The data are available from December 1957 to yesterday and they are updated daily after 6PM (Arpa Piemonte, 2017). To obtain this grid, ARPA Piemonte processed the data from the single point-stations with a statistical methodology based on the technique of "optimal interpolation" (Arpa Piemonte, 2010). The grid has a spatial resolution of 15 km and the interpolated value for each cell is the mean of all the values from the stations present in that cell.

To obtain the temporal series to use in the validation, the timeseries 2006-2020 of data corresponding to the cell containing the center of the cell selected for the models' output were extracted.

2.2 Climate projections for RCP2.6 and RCP8.5 scenarios

Two climate scenarios (RCP2.6 and RCP8.5) were considered in this study, coming from several climate models, to take into account the uncertainty of climate projections. For each of the two scenarios, daily timeseries of precipitation, minimum temperature and maximum temperature were retrieved from the selected datasets.

2.2.1 Climate scenarios

In *Guidance for EURO-CORDEX climate projections data use* published by the EURO-CORDEX community (2021), climate scenarios are defined as “representations of various possible future states of the climate system, based on numerical model simulations”. RCPs (Representative Concentration Pathways) in particular are scenarios developed for the IPCC Assessment Report (AR5) and represent pathways of the additional radiative forcing caused by anthropogenic activity till the end of the 21st century (the value in 1750 is considered as reference) (EURO-CORDEX community, 2021).

There are four RCPs. From the “most positive” to the “worst” one they are:

- RCP2.6;
- RCP4.5;
- RCP6.0;
- RCP8.5.

The number indicates the approximate total radiative forcing (W/m^2) in year 2100 relative to 1750 reached by each scenario. They represent a range of possible 21st century climate policies, with RCP2.6 being the mitigation scenario leading to low forcing level, RCP4.5 and RCP6.0 being two stabilization scenarios and RCP8.5 representing the scenario in which no climate policies are implemented resulting in the highest greenhouse gases emissions. Table 2.1 summarizes the main characteristics of these four scenarios. To consider the full range of possibilities in this study, the most positive (RCP2.6) and negative (RCP8.5) scenarios in terms of climate change magnitude were taken.

Table 2.1: Summary of the main characteristics of RCPs (IPCC, 2021).

Representative Concentration Pathway (RCP)	Forcing compared to 1750 [W/m^2]	Climate policy associated with the scenario	Projected global average temperature increase from 1986-2005 ($^{\circ}\text{C}$)
2.6	2.6	Mitigation	1.0
4.5	4.5	Stabilization	1.8
6.0	6.0	Stabilization	2.2
8.5	8.5	None	3.7

2.2.2 Climate models

The focus of this work was a local study of climate change impacts on the agriculture of a small area in Piemonte, Italy. For this reason, the research for available future climate projections datasets focused on those with a small enough resolution to represent the local scale.

A research of all the products available on the internet was performed, focusing on the smallest grid resolutions available and the European (EUR) region (Appendix I for the details on the products found). From all the datasets found openly available, the *CORDEX regional climate model data on single levels* dataset from the Climate Data Store (CDS, 2022) was chosen, because it has one of the better resolutions ($0.11^{\circ}\times 0.11^{\circ}$) and all the climate variables needed (precipitation and temperature) for both RCP2.6 and RCP8.5. Specifically, the three variables selected to be used are, as describe by Copernicus Climate Change Service:

- *Mean precipitation flux* ($\text{kg m}^{-2} \text{s}^{-1}$), “the deposition of water to the Earth's surface in the form of rain, snow, ice, or hail. The precipitation flux is the mass of water per unit area and time. The data represents the mean over the aggregation period” (C3S, 2022b).
- *Maximum 2m temperature in the last 24 hours* (K), “the maximum temperature of the air near the surface. The data represents the daily maximum at 2m above the surface” (C3S, 2022b).
- *Minimum 2m temperature in the last 24 hours* (K), “the minimum temperature of the air near the surface. The data represents the daily minimum at 2m above the surface” (C3S, 2022b).

CORDEX regional climate model data on single levels is an entry on the CDS (2022) that collects downscaled regional climate projections for all CORDEX domains, including EURO-CORDEX (Jacob et al., 2014), the one interesting for this work. CORDEX stands for COordinated Regional Downscaling Experiment and it consists in “a WCRP framework to evaluate regional climate model performance through a set of experiments aiming at producing regional climate projections” (WCRP, 2022). The experiments carried out under this framework used Regional Climate Models (RCMs) to downscale Global climate models (GCM) simulations using the GCMs output data as lateral boundary conditions (EURO-CORDEX community, 2021). It is a process called dynamical downscaling and it is one of the two common downscaling technique, together with the empirical-statistical downscaling (ESD). Projects like CORDEX are very important nowadays considering that adaptation strategies should be based on climate change impacts that may occur on regional and national scales. So, there is a strong need for smaller scale climate projections to implement the local impact models. The EURO-CORDEX ensemble (Jacob et al., 2014) considered those CORDEX experiments run on the EURO domain. The EURO-CORDEX ensemble is based on RCPs and EURO-CORDEX models are operated on the spatial scales of approximately 12 km or 50 km (EURO-CORDEX community, 2021).

Data series of the three variables described above at the finest resolution of 0.11° (~ 12.5 km; EUR-11) for the two scenarios RCP2.6 and RCP8.5 were retrieved from the EURO-CORDEX CMIP5 simulations (Jacob et al., 2014) available on the Climate Data Store (CDS, 2022). The period considered is 2006-2055, subdivided into two sub-periods, the validation one 2006-2020 and the future 2021-2055 in the performed analysis. Combinations of three GCMs (Table 2.2) and three RCMs (Table 2.3) part of the EURO-CORDEX ensemble were retrieved, which form the 10 datasets (5 for RCP2.6 and 5 for RCP8.5) reported in Table 2.4 .

Table 2.2: Global Climate Models used in this work

Model name	Reference	Institution
ICHEC-EC-EARTH	Hazeleger et al. (2010)	Irish Centre for High-End Computing EC-Earth Consortium
MPI-M-MPI-ESM-LR	Giorgetta et al. (2013)	Max Planck Institute for Meteorology
NCC-NorESM1-M	Bentsen et al. (2013)	Norwegian Earth System Model

Table 2.3: Regional Climate Models used in this work

Model name	Reference	Institution
CLMcom-CCLM4-8-17	Baldauf et al. (2011)	Climate Limited-area Modelling Community (CLM-Community)
KNMI-RACMO22E	van Meijgaard et al. (2008)	Royal Netherlands Meteorological Institute
SMHI-RCA4	Strandberg et al. (2014)	Swedish Meteorological and Hydrological Institute, Rossby Centre

Table 2.4: List of the combinations of global and regional models used for the climate projections, together with the abbreviation used in this work

Scenario Abbrev.	RCM	GCM	Time interval
<i>RCP26-M1</i>	CLMcom-CCLM4-8-17	ICHEC-EC-EARTH	2006-2020 2021-2055
<i>RCP26-M2</i>	KNMI-RACMO22E	ICHEC-EC-EARTH	2006-2020 2021-2055
<i>RCP26-M3</i>	SMHI-RCA4	ICHEC-EC-EARTH	2006-2020 2021-2055
<i>RCP26-M4</i>	SMHI-RCA4	NCC-NorESM1-M	2006-2020 2021-2055
<i>RCP26-M5</i>	KNMI-RACMO22E	MPI-M-MPI-ESM-LR	2006-2020 2021-2055
<i>RCP85-M1</i>	CLMcom-CCLM4-8-17	ICHEC-EC-EARTH	2006-2020 2021-2055
<i>RCP85-M2</i>	KNMI-RACMO22E	ICHEC-EC-EARTH	2006-2020 2021-2055
<i>RCP85-M3</i>	SMHI-RCA4	ICHEC-EC-EARTH	2006-2020 2021-2055
<i>RCP85-M4</i>	SMHI-RCA4	NCC-NorESM1-M	2006-2020 2021-2055
<i>RCP85-M5</i>	KNMI-RACMO22E	MPI-M-MPI-ESM-LR	2006-2020 2021-2055

The choice of these combinations GCM-RCM was made selecting between all the possibilities those that answered the needs of this study (i.e., daily value of precipitation, maximum and minimum temperature; both the two climate scenarios available), performed better in the validation carried out by the Climate Data Store (C3S, 2022a), and have the same characteristics of spatial grid and time variable (so to have comparable results).

Chapter 3 Case study and preliminary analyses

3.1 The area of interest

The area considered is part of the Cuneo district, in the Region of Piemonte, Italy.

Piemonte is a region in the north-west of Italy. Historically, it has always been a region rich in water. This is a Region where irrigation for agriculture is well developed and common. Through a census took by the Region about 10 000 km of canals connected to the primary system were mapped, to which over 2000 km of pressured irrigation pipelines can be added (Regione Piemonte, n.d.).

The Cuneo district presents some specific characteristics that made it interesting for this study. It suffers from irrigation water supply problems, more severe than the other districts of the Region. This is mainly due to the fact that the rivers on which it depends originate from the south-west of the Alps, a region without significant glaciers, so there is no certain water supply after the snowmelt. Furthermore, the management of the irrigation system is very fragmented between tens of unions, and this makes it difficult organizing strategies to face the more and more frequent water crises (Regione Piemonte, n.d.). In this context, an analysis of water balances related to irrigation and how the scenario may change due to climate change is of sure importance.

To have an idea of the current situation of the area, a preliminary analysis of agricultural practices and data was performed. The area considered is the one of 28 municipalities under the Cuneo district, shown in Figure 3.1: Briga Alta, Beinette, Boves, Borgo San Dalmazzo, Castelletto Stura, Centallo, Chiusa di Pesio, Cuneo, Entracque, Fossano, Frabosa Soprana, Frabosa Sottana, Limone Piemonte, Margarita, Mondovì, Montanera, Morozzo, Peveragno, Pianfei, Roaschia, Robilante, Rocca de' Baldi, Roccaforte Mondovì, Roccavione, Sant'Albano Stura, Valdieri, Vernante, Villanova Mondovì.

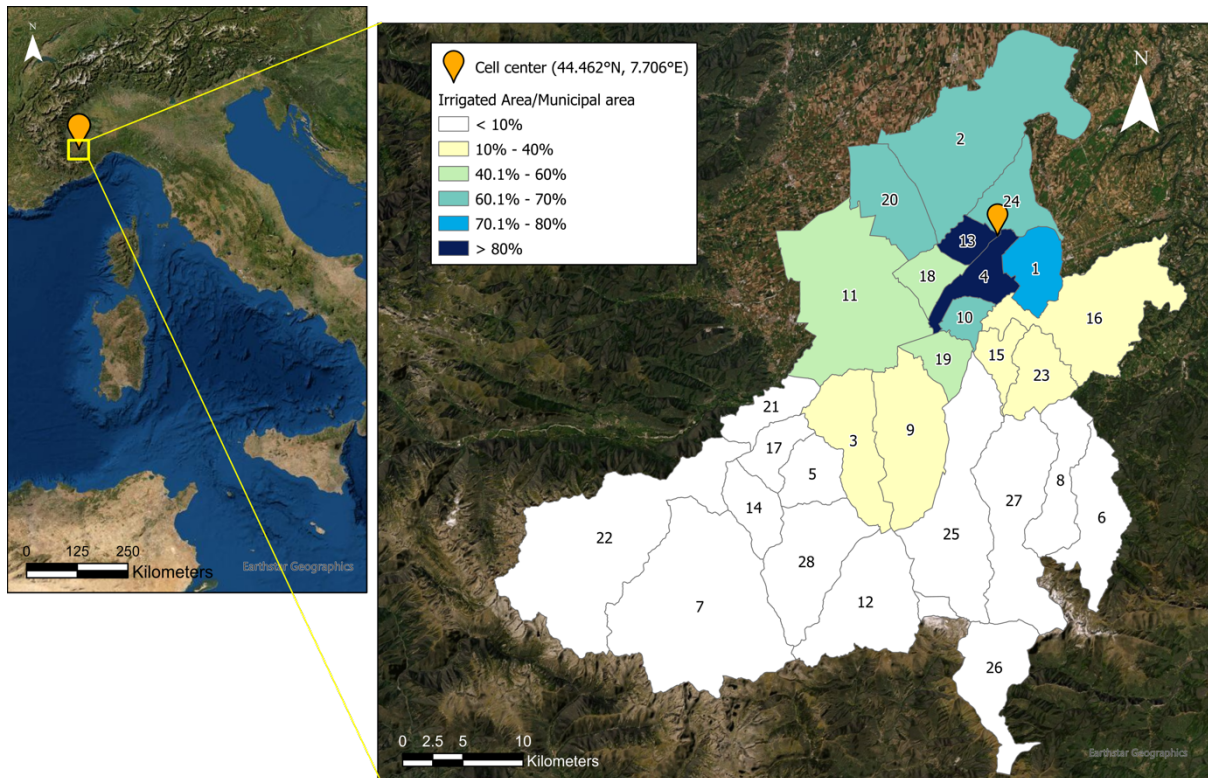


Figure 3.1: The area of interest in the north-west of Italy, with the detail for each municipality of the percentage of irrigated area over the total municipal area. Legend of municipalities: Rocca de' Baldi(1), Fossano(2), Boves(3), Morozzo(4), Robilante(5), Frabosa Soprana(6), Entracque(7), Frabosa Sottana(8), Peveragno(9), Margarita (10), Cuneo(11), Limone Piemonte(12), Montanera(13), Roaschia(14), Pianfei(15), Mondovì(16), Roccavione (17), Castelletto Stura(18), Beinette (19), Centallo (20), Borgo San Dalmazzo (21), Valdieri (22), Villanova Mondovì (23), Sant'Albano Stura (24), Chiusa di Pesio (25), Roccafortè Mondovì (27), Briga Alta (26), Vernante(28).

These municipalities were chosen as they are part of the project ALCOTRA, in particular of the PITER ALPIMED strategy (ALPIMED, n.d.). One of the objectives of this strategy is to study the water resources of the area and the water use of the different economic activities, also in the context of climate change, to foster better knowledge and capability of adaptation in the mountain communities. This work follows the same aims, with the hope of constituting a further resource for more efficient adaptation plans in the area.

This territory has a total population of 175 226 people, 30% of the total population of the Cuneo district (ISTAT, 2010), and it covers a total area of 152 951 ha (1529.51 km²), 22% of the district. As reported by the 6th census of agriculture carried out by ISTAT (2010), 40% of this total surface was cultivated (utilized agricultural area, UAA) in 2010, a percentage that became 22% if only the irrigated cultivated area is considered (irrigated UAA). Table 3.1 reports the

summary of this useful parameters. The 22% of irrigated UAA over the total municipal area is a value obtained averaging the very different situations of each municipality. As Figure 3.1 shows, the territory can be roughly subdivided into two parts, the municipalities on higher altitudes with less than 10% of irrigated hectares, and the municipalities in the valley with more than 10% of irrigated lands (with Montanera and Morozzo reaching peaks of over 80%).

Table 3.1 Summary of significant parameters

Total surface (ha)	UAA (ha)	Irrigated UAA (ha)	$\frac{\text{Irrigated UAA}}{\text{municipal area}}$ (%)
152 951	60 558.31	33 754.78	22%

In the next graphs the agricultural sector of the area is described more in detail. All the data used for the elaborations were taken from the dataset of the 6^o *censimento dell'agricoltura* (6th census of agriculture) by ISTAT (2010).

In Figure 3.2 the percentages of hectares cultivated for specific crops over the total 33 754.78 hectares of irrigated UAA are shown. Covering 36% of irrigated UAA, maize is the main irrigated crop (a share that reaches 46% if also green maize is considered). The other main crops cultivated in the area are fodders, pastures, cereals, and fruit trees, but none of these category reaches the high percentage of maize. Furthermore, arable crops are the most irrigated between the crop typologies (85% of the UAA of arable crops is irrigated), as depicted in Figure 3.3. Lastly, maize is also the crop for which the most water for unit of area is used for irrigation (Figure 3.4). Therefore, maize was chosen as the crop in input for the model computations of this study.

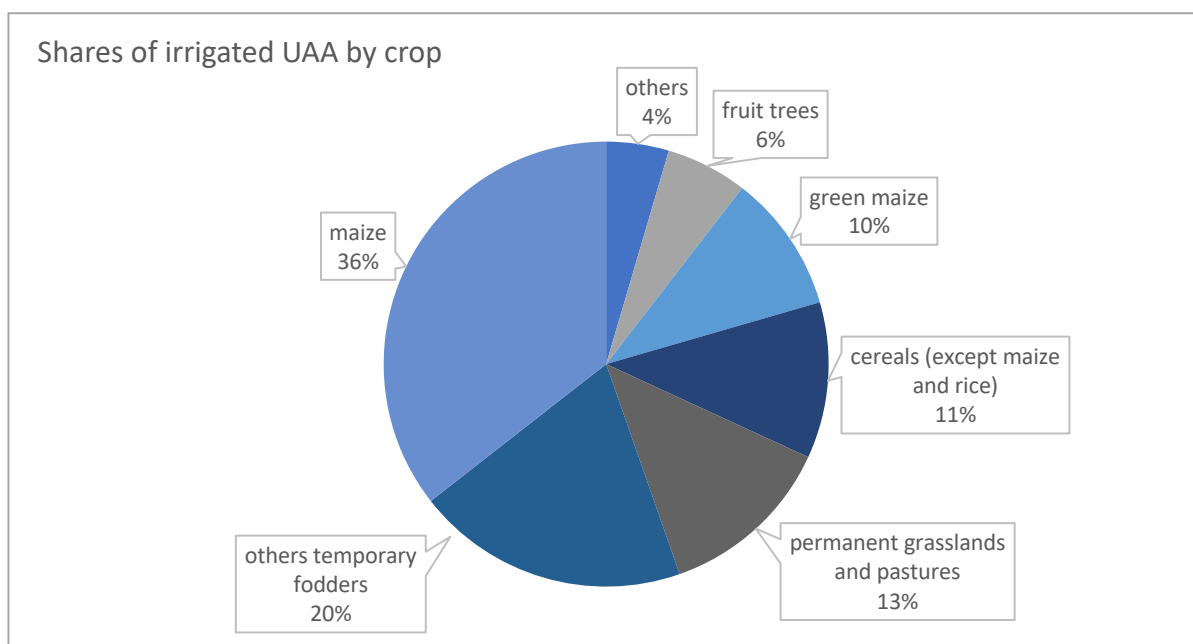


Figure 3.2: Shares of Irrigated Utilized Agricultural Area (UAA) for each crop. 'Others' includes all the crops with less than 1000 ha of cultivated land. Source: elaboration of ISTAT data (2010).

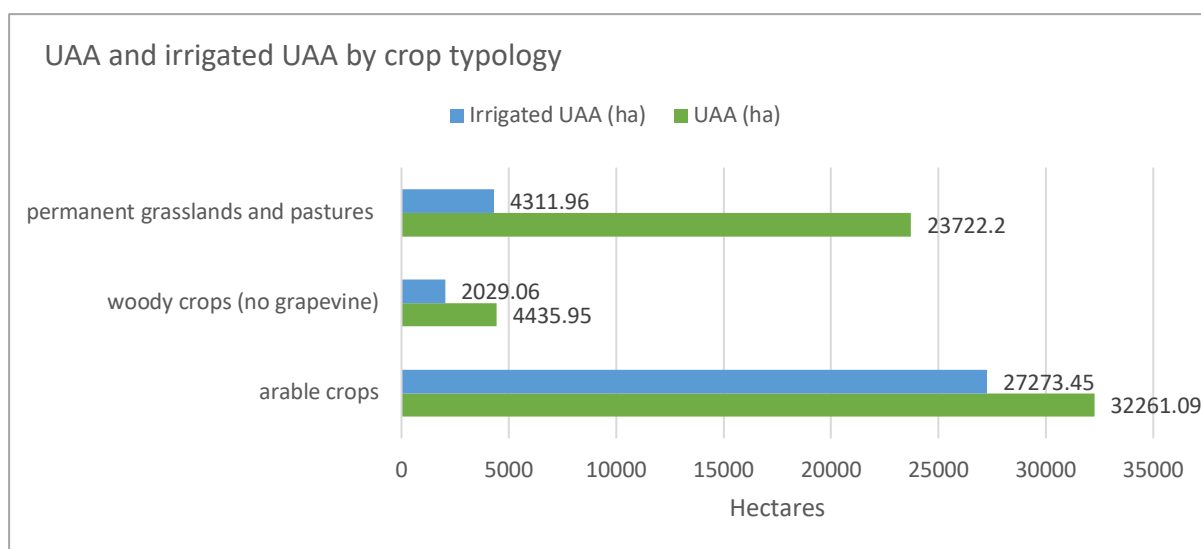


Figure 3.3: UAA and Irrigated UAA by crop typology in hectares. 'Arable crops' includes all cereals (maize included). Source: elaboration of ISTAT data (2010).

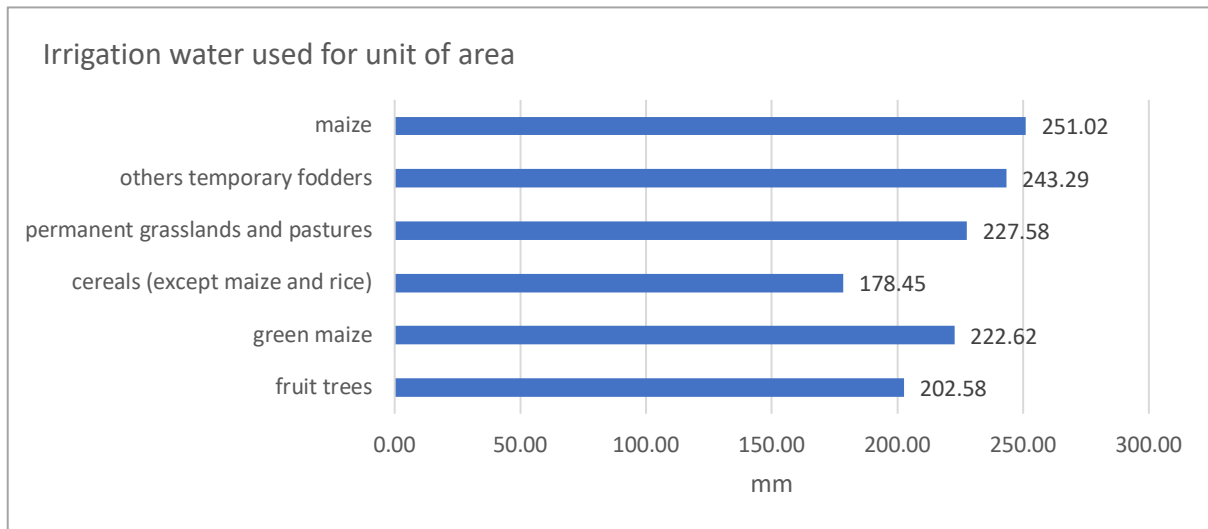


Figure 3.4: Water used for irrigation (mm) for unit of area by crop typology. Source: elaboration of ISTAT data (2010).

Given all the previous considerations, it is clear the importance of studying the irrigation requirements and water cycle of the area, in order to help the adaptation of its agricultural sector to the effects of climate change. In this study, with irrigation requirements it is meant the amount of water needed by the crop to satisfy its evapotranspiration demand when precipitation is not sufficient.

3.1.1 Selection of temporal series

An important step performed was to select from the European grid provided by the CDS for each model, a cell representative for the whole local area studied, since in this study it was decided not to analyze the spatial variation but only the temporal variation of the variables.

All the models selected provide the data in netCDF files. Each of these files contains two bi-dimensional variables *lat* and *lon* within which the information on latitude and longitude of each cell of the spatial grid is stored in the form of curvilinear geographic coordinates. Those are the coordinates of the center of each cell, as shown in Figure 3.5.

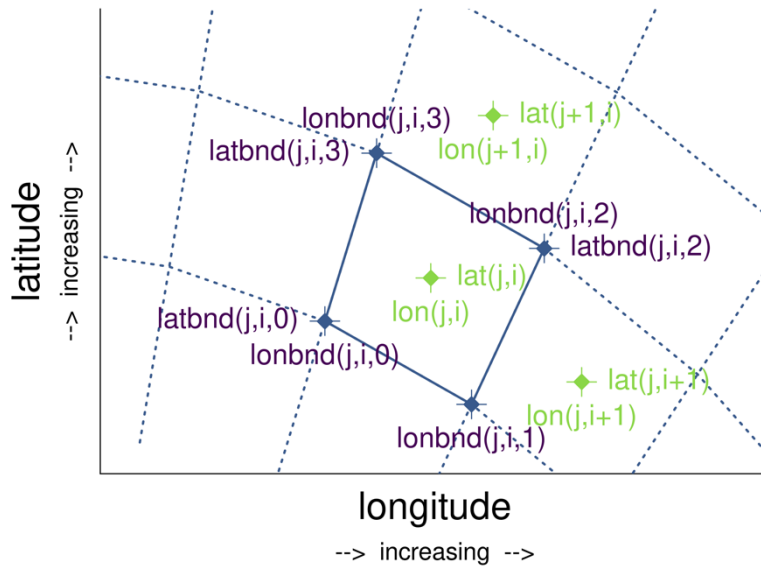


Figure 3.5: Scheme of netCDF spatial grid coordinates in the case of two-dimensional horizontal coordinate axes (Eaton et al., 2021).

In some cases, also two other variables are provided, called *lat_vertices* and *lon_vertices*, which contains the coordinates of the cells' vertices. In *NetCDF Climate and Forecast (CF) Metadata Conventions* by Eaton et al. (2021) it is possible to read:

"In the case where the horizontal grid is described by two-dimensional auxiliary coordinate variables in latitude $lat(n,m)$ and longitude $lon(n,m)$, and the associated cells are four-sided, then the boundary variables are given in the form $latbnd(n,m,4)$ and $lonbnd(n,m,4)$, where the trailing index runs over the four vertices of the cells."

The indices n and m are in this case *r lon* and *r lat*, the longitude and the latitude respectively of the 90° rotate grid on which the data are provided.

To select the reference cell the following procedure was performed:

- Firstly, the coordinate range related to the area of study was individuated, from 44.31°N to 44.62°N and from 7.47°E to 7.90°E.
- Then a precise point with coordinates 44.44°N - 7.64°E was arbitrarily selected as reference inside this range, since placed in the most intensely cultivated area.
- From all the cell of the spatial grid of the models' outputs that fell inside the range, the cell chosen was one placed on an intensely irrigated and cultivated area with the coordinates closer to the reference point.

The center of cell selected with this procedure has the coordinates: 44.462°N, 7.706°E. The point is signaled by the orange placemark in Figure 3.1 and depicted in detail together with the coordinates of the cell's vertices in Figure 3.6. The area of the selected cell covers part of the territory of the most intensively cultivated municipalities of the area of study, which are Morozzo, Montanera, and Sant'Albano Stura (Figure 3.6).

Selected cell

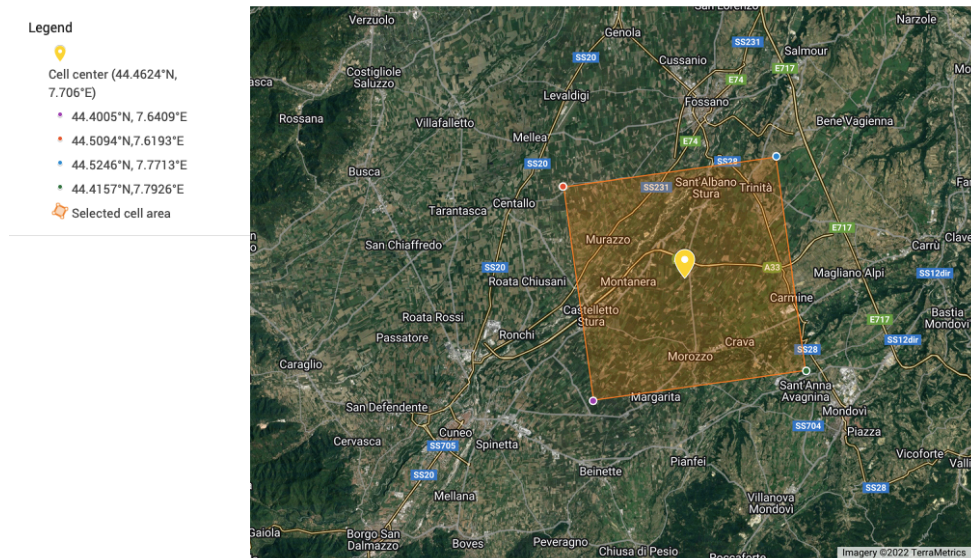


Figure 3.6: Google Map which enlightens the placement of the cell selected for the study (Google, n.d.).

3.2 Validation

Before proceeding with the crop model calculations, the validation of precipitation, maximum and minimum temperature is performed to assess the ability of the models' projections to represent the specific reality of the local area. This step is important since model outputs have inevitably a bias when compared to the reference data sets, due to the complex nature of the climate system, model errors and approximations. For this reason, in this study it was used a multi-model multi-scenario ensemble (i.e., several models and two scenarios) instead of a single output. This choice was made coherently with what is suggested by Kreienkamp et al. in *Good practice for the usage of climate model simulation results - a discussion paper* (2012): "Since there is no single 'optimal' model, the analysis of a number of simulations (ensemble) is a scientifically suitable strategy to describe the range of climate changes that can be expected".

The validation was performed on all the five GCM-RCM couples and both the scenarios RCP2.6 and RCP8.5.

3.2.1 Minimum and maximum temperature

The validation of the temperature datasets was performed plotting the scatter plots between the total precipitation for each month of the period projected by the model (x_{scenario}) and the total precipitation of each month from ARPA observations ($x_{\text{observations}}$). The plots for the validation of RCP2.6-M3 and RCP8.5-M3 are depicted in Figure 3.7 as an example of the procedure which has been repeated for all the five models and both the climate scenarios. Together with the scatter plot, also the bisector of the quadrant and the linear fitting line are shown. The resulting coefficients for the different models evaluated for both T_{min} and T_{max} are collected in Table 3.2. The closer a is to 1 and the closer b is to 0, the better is the fitting of the models' output to the observations.

The majority of the datasets showed a shift of the temperature projections compared to the observations, demonstrated by the positive values of the b coefficient (negative in the case of M1) being often more than 3. Therefore, a bias correction procedure has been performed for all the models and scenarios. Appendix II reports all the validation graphs for each dataset analyzed.

Table 3.2: Coefficients a and b of the linear interpolation used to perform the bias correction for T_{max} and T_{min}

	T_{min}		T_{max}	
	a	b	a	b
RCP26-M1	0.922	-0.163	0.804	4.64
RCP26-M2	0.874	4.46	0.836	5.46
RCP26-M3	1.01	1.66	0.812	3.93
RCP26-M4	1.01	0.145	0.862	1.69
RCP26-M5	0.838	3.2	0.79	5.25
RCP85-M1	0.988	-0.912	0.846	4.06
RCP85-M2	0.946	3.77	0.927	3.88
RCP85-M3	1.06	1.34	0.871	3.17
RCP85-M4	1.03	0.0904	0.899	0.752
RCP85-M5	0.887	2.41	0.852	3.72

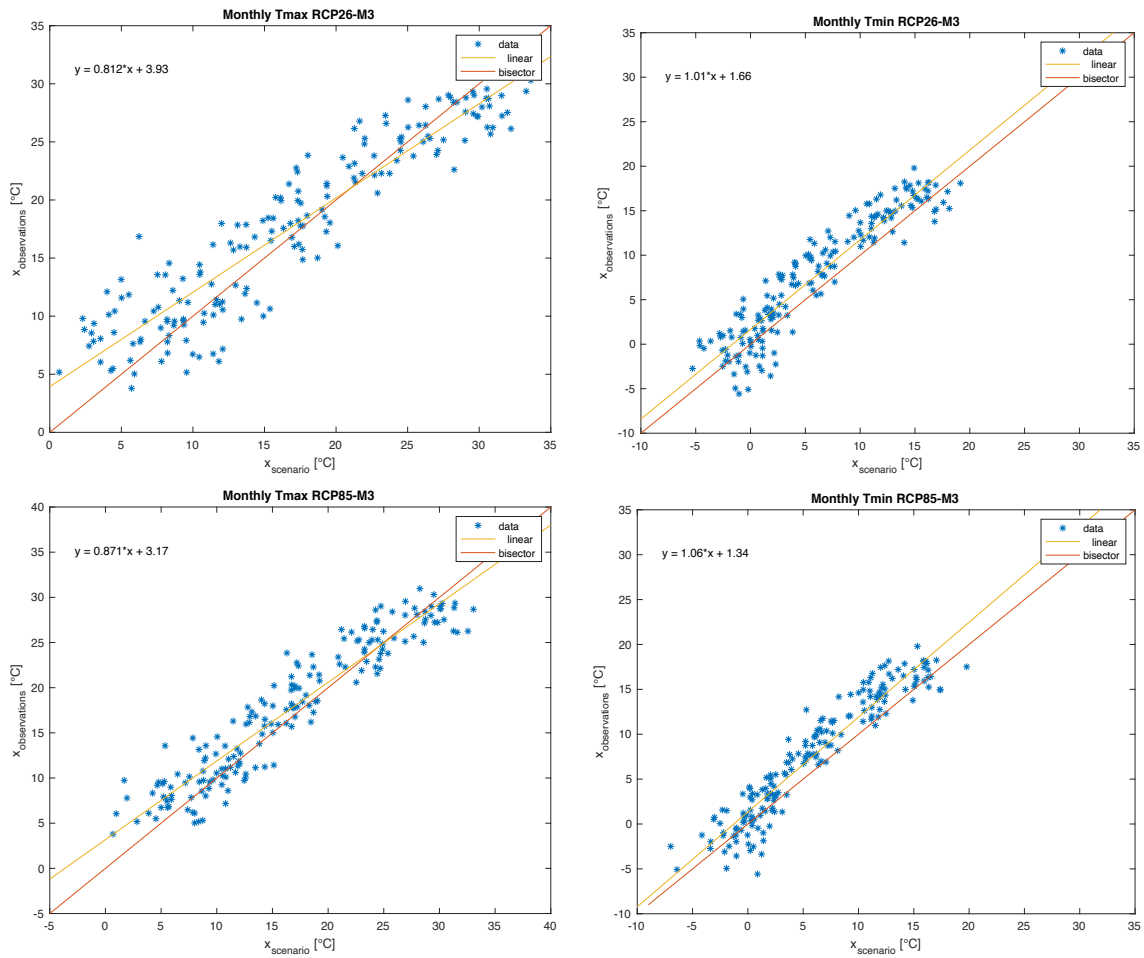


Figure 3.7: Validation graphs for RCP2.6-M3 (top) and RCP8.5-M3 (bottom), both Tmax (left) and Tmin (right). The line of the linear interpolation and its equation, as well as the bisector of the quadrant, are shown.

3.2.2 Precipitations

For the precipitations, the annual mean regimes were considered since the scatter plots of monthly total precipitation (model output versus ARPA piemonte data for 2006-2020 period) did not give useful indication on the quality of the series. With precipitation regime it is meant the mean of monthly total precipitation calculated for each month for the 15 years (e.g., the value for January is the mean between all the totals for January from 2006 to 2020). Doing so, it is possible to appreciate the yearly behavior of monthly precipitation, with higher values in spring and winter, and lower values in summer. All the models represent more or less this behavior of the variable, but some of them severely underestimate the phenomenon systematically and so required a bias correction. The datasets that were bias corrected were

M1, M3 and M4 for both the RCPs. As an example of the underestimation of the observations of these models (and the type of graphs obtained with this validation procedure), the plots for RCP2.6-M3 and RCP8.5-M3 are shown in Figure 3.8. For the depiction of all the plots for the ten climate datasets, see Appendix III.

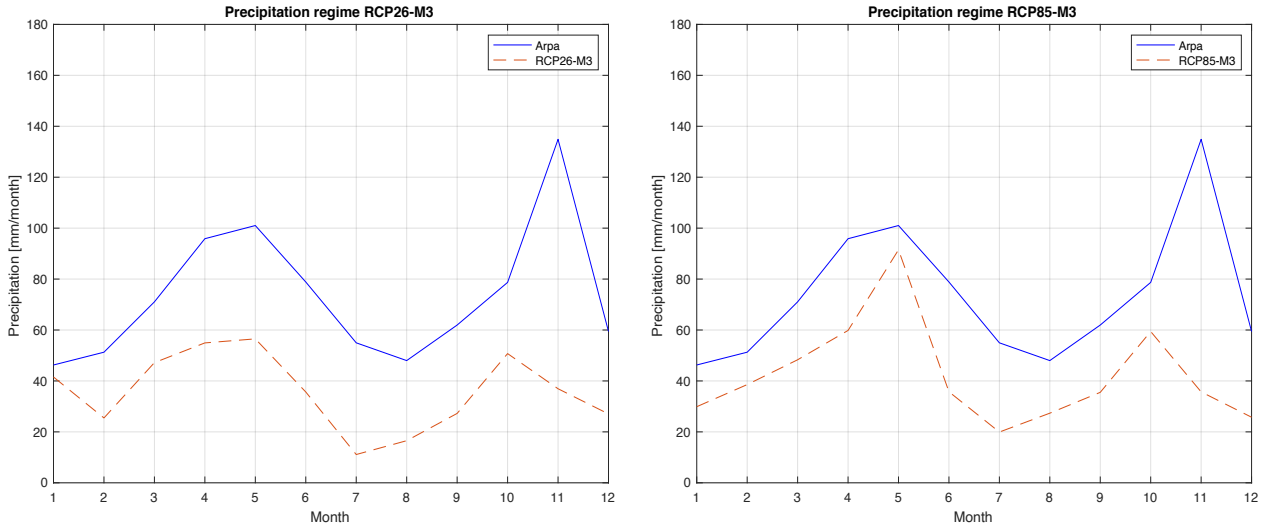


Figure 3.8: Comparison between the precipitation regime (average monthly precipitation) of RCP26-M3 (left) and RCP85-M3 (right) and the regime showcased by the Arpa Piemonte observations (Arpa Piemonte, 2017) from 2006 to 2020.

3.3 Bias Correction

As illustrated before, some datasets show some differences between the model's output and the reality. Before calculating ET_0 from T_{max} and T_{min} then, these timeseries have been bias corrected both for the period 2006-2020 and 2021-2055. The method used was the following:

$$T_{BC} = a * T_{scenario} + b \quad (3.1)$$

where T_{BC} represents the matrix of bias corrected daily values, $T_{scenario}$ is the matrix of original daily values from the model and a and b are the two coefficients estimated by linear fitting at the minimum squares shown in Table 3.2.

For precipitations, a linear scaling was performed as illustrated by the following equation (Fang et al, 2015):

$$P_{BC,i,m} = P_{scenario,i,m} * \frac{P_{obs,m}}{P_{scen,m}}$$

(3.2)

where $P_{BC,i,m}$ is the bias corrected value for the i -day of month m , $P_{scenario,i,m}$ is the original value for the i -day of month m , $P_{obs,m}$ and $P_{scen,m}$ are the mean values of total month precipitation over the years for the observations and the model respectively.

For example, Figure 3.9 illustrates the results of precipitations bias correction of M3 for both the scenarios. The procedure applied has strong effects on the characteristics of the future series especially, generating in some cases peaks which were not present in the original series (Figure 3.9). However, the main features of the series were maintained, with peaks in spring and winter and less rainfalls in summer. Furthermore, for the future series the focus of the bias correction was more on correcting the shift in terms of order of magnitude of those models that showed an important bias, than obtaining values equal to the observations (since clearly the future values will be different than the historical series). Having said so, this bias correction procedure was judged sufficient for the scope of the study.

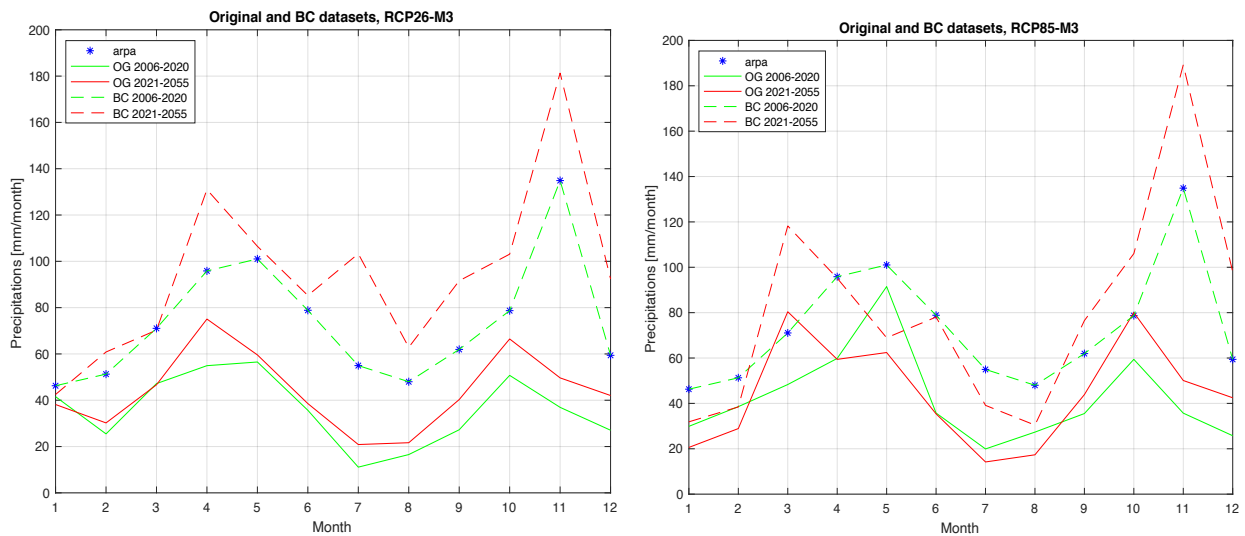


Figure 3.9: Mean annual precipitations regime of original and bias corrected data of M3, both RCP2.6 (left) and RCP8.5(right)

3.4 Variables trends analysis

The time series of the three variables after the bias correction are then analyzed, to have an idea of what the climate is projected to be from 2006 to 2055 in the studied area, according to the

climate datasets considered. When the plots represent the ensemble mean, it means the average between the data from the five datasets for RCP2.6 or for RCP8.5 scenarios.

In particular, the trends in precipitations and temperature will be represented with a focus on the three summer months of June, July and August. Summer is the main season for maize development and also coincides with the main irrigation period, since irrigation is required during these three months due to the low precipitations. Being the focus of this work studying the effect of climate change on future irrigation requirements, analyzing the future trends of climate variables in the summer is needed to be able to fully understand the outputs of the crop model. September was not included in the summer months for this analysis because the precipitations and temperatures of the second half of the month do not affect maize growth, since it is harvested on the 15th of September. It was preferred to analyze together only months which are completely part of the growing season of maize.

3.4.1 Precipitations

Firstly, the trend of total annual precipitation from 2006 to 2055 was plotted (Figure 3.10). The inter-annual variability for both the RCP scenarios is high and there are no visible periodicities. In Figure 3.10 the values for each dataset were plotted together with their ensemble mean, to show the variability inside the ensemble. The aim of using an ensemble of climate models is to describe the range of climate changes that can be expected. However, only the ensemble mean will be represented from now on, for the sake of clarity of the graphs and of the analysis. It is still important to keep in mind the range of variability from which the mean originates. The average value of total annual precipitations for the period 2006-2020 obtained from Arpa Piemonte observations is almost 900 mm/year, and the bias corrected series here presented are coherent with this order of magnitude.

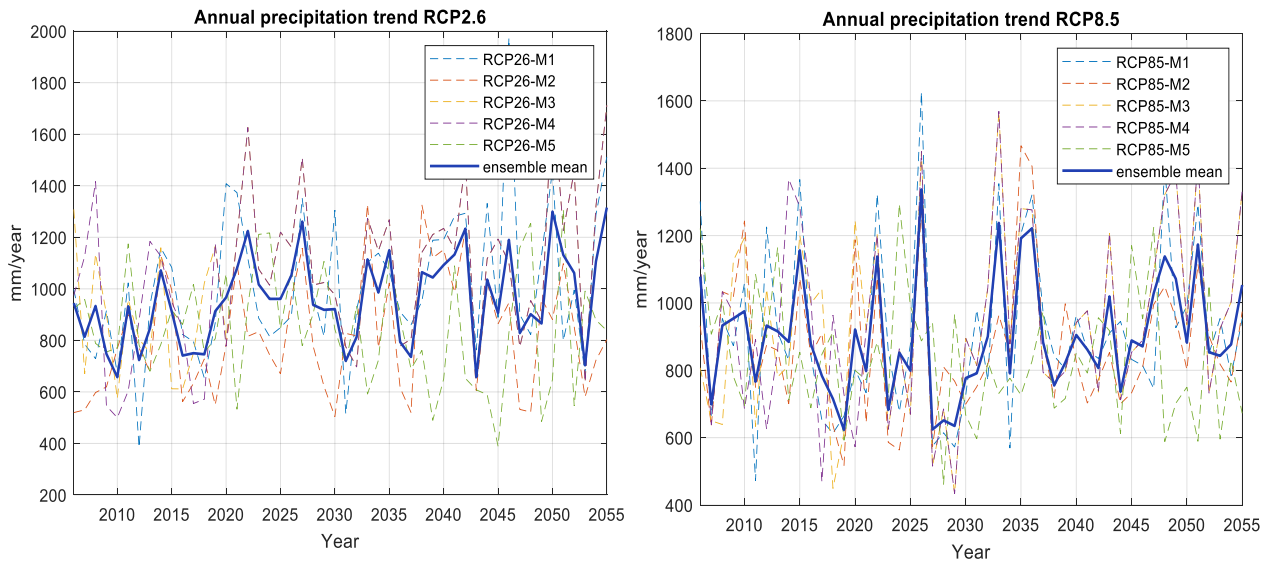


Figure 3.10: Total annual precipitation (mm/year) series from 2006 to 2055, all the datasets plotted, and the ensemble mean, for RCP2.6 (left) and RCP8.5 (right).

As said previously, the most important season for maize development is summer, so it is interesting to see also which is the trend of precipitations for the particular months of June, July, and August. The plots presented in Figure 3.11 shows the different behaviour of the variable in the two climate scenarios. Considering RCP2.6, there is an increase of precipitations from 2006 to 2055, while in RCP8.6 scenario precipitations are projected to decrease, even though the inter-annual variability remains high.

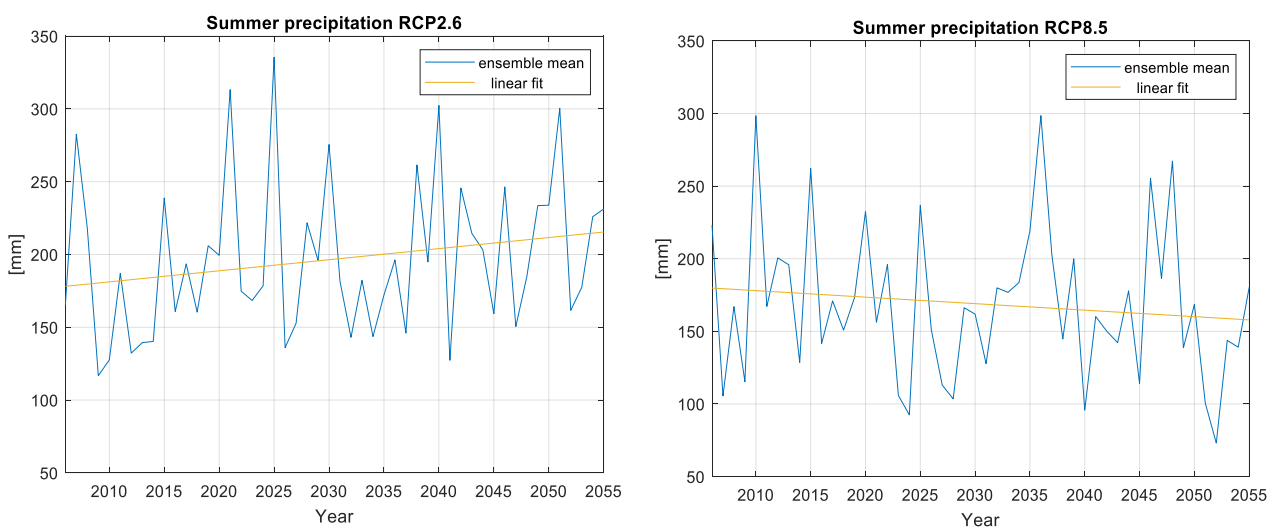


Figure 3.11: Summer (June, July and August) total precipitations trend from 2006 to 2055 (ensemble mean and linear fit), for RCP2.6 (left) and RCP8.5 (right)

3.4.2 Temperature

After having seen how, in the future, precipitations will increase or decrease depending on the climate scenario considered, now it is the turn of the two temperature variables, T_{max} and T_{min} . Again, in Figure 3.12 the trend from 2006 to 2055 of the average monthly summer temperature (considering June, July, and August) is shown for both the climate scenarios. As explained before, these three months were chosen because they are the most critical for the growth of maize in the area, during which reference evapotranspiration and actual evapotranspiration are usually higher (see next section 3.5 and Chapter 4 for the analysis of ET_0 and ET_a respectively), while September was left out because it is not completely part of maize growing season. The mean temperature was computed from T_{max} and T_{min} values and then plotted to have a better visual representation of the situation. Under RCP2.6 hypothesis, the temperature remains almost constant (no significant increasing or decreasing trend), while under RCP8.5 conditions there is a visible increase of the variables from 2006 to 2055.

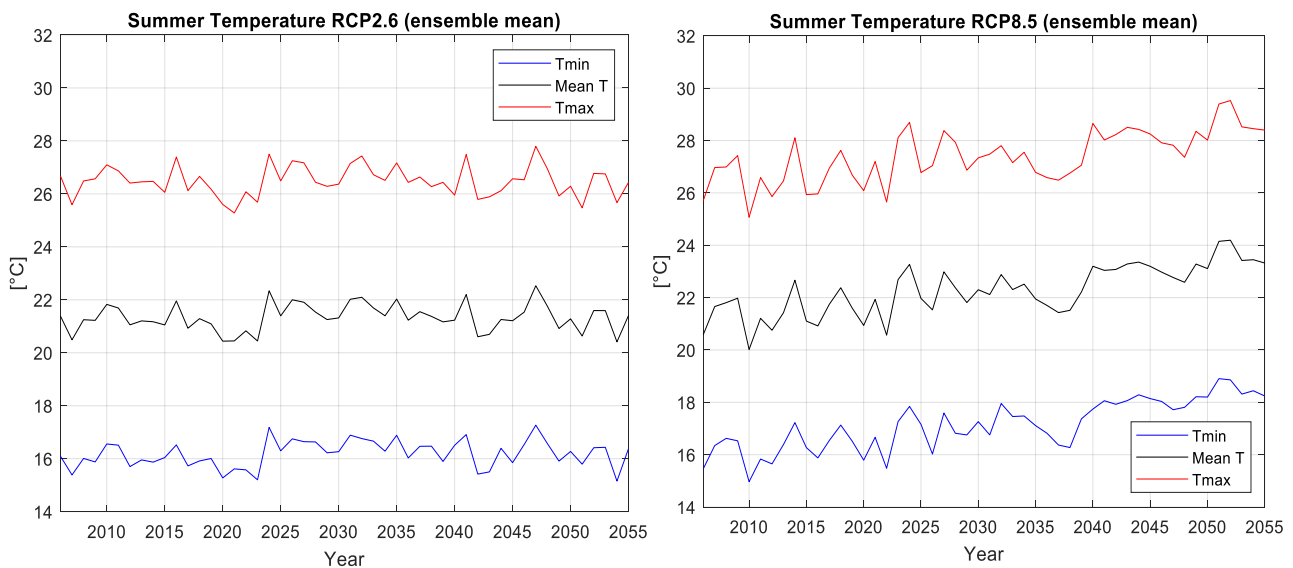


Figure 3.12: Summer (June, July and August) averages of T_{min} , T_{max} and mean temperature, from 2006 to 2055 (ensemble mean), for RCP2.6 (left) and RCP8.5 (right)

The increase in temperatures towards the end of the future period could lead reference evapotranspiration to rise and so maize water needs could be expected to rise too in the future. Assessing quantitatively the increase in irrigation requirements generated by these future trends in precipitations and temperature will be the aim of the crop model's runs performed in this study.

3.5 Reference evapotranspiration

In this study, the daily ET_0 (mm/day) was calculated with the Hargreaves-Samani method (Hargreaves et al., 1985) with the equation:

$$ET_{0,i} = k_{HS} \cdot R_{a,i} \cdot (T_i + 17.8) \cdot \sqrt{T_{max,i} - T_{min,i}} \quad (3.3)$$

where $T_{max,i}$, $T_{min,i}$ and T_i are respectively the maximum, minimum and mean temperature of the i -day ($^{\circ}\text{C}$); k_{hs} is an empirical coefficient (-); and $R_{a,i}$ is the equivalent evapotranspiration (mm/day).

T_{min} and T_{max} dataserries consist in the bias corrected values of the datasets provided by the climate models. The mean temperature T_i was obtained from the maximum and minimum temperature as follows:

$$T_i = \frac{T_{max,i} + T_{min,i}}{2} \quad (3.4)$$

k_{hs} is fixed to the value specified by Hargreaves-Samani: $k_{hs}=0.0023$. $R_{a,i}$ depends on the latitude of the area considered, so the latitude ϕ of the center of the specific cell studied was selected: $\phi = 44.4624^{\circ}\text{N} = 0.7760$ rad.

The results of the calculation for each model were then plotted to assess the quality of the procedure and to analyze the evolution of ET_0 in time. Figure 3.14 and Figure 3.13 show the plots for the two periods 2006-2020 and 2045-2054, for RCP2.6 and RCP8.5 respectively (a 7-days moving mean was applied to all the series for clearer plots). All the resulting ET_0 series show the typical “bell” shaped curve of daily values from the start to the end of the year, but with some differences from dataset to dataset. The differences are mainly evident during the summer period, while going earlier and later in the year all the datasets get closer to the ensemble mean. An increase of ET_0 from 2006 to 2055 is projected, especially under RCP8.5 hypothesis, consistently with the increase in temperatures projected for the future period.

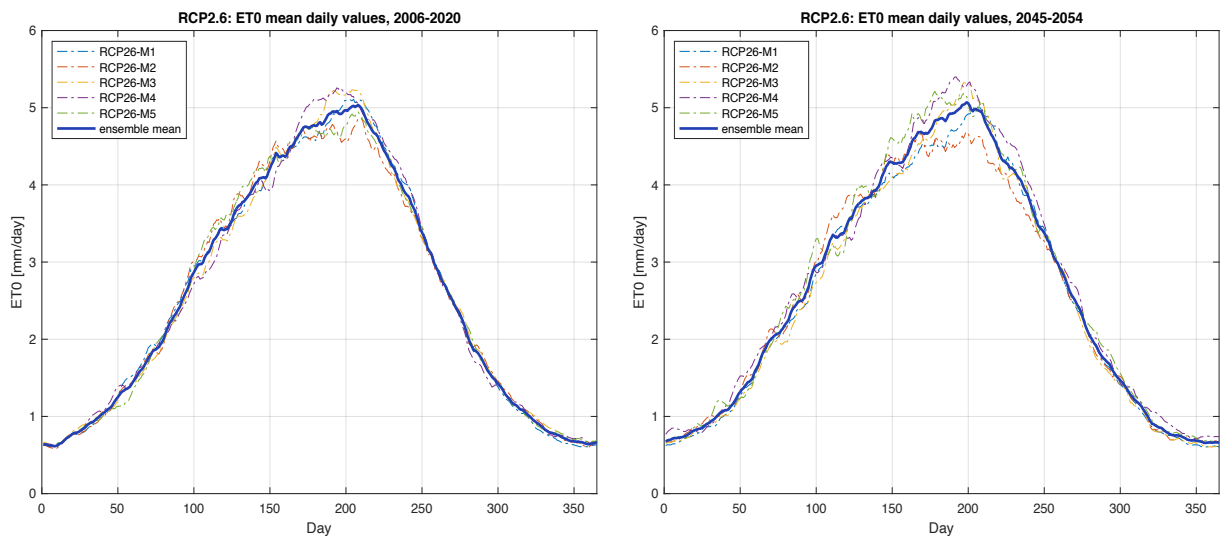


Figure 3.14: Reference evapotranspiration annual behaviour for the present period (2006-2020, left) and the future decade 2045-2054 (right), RCP2.6 scenario.

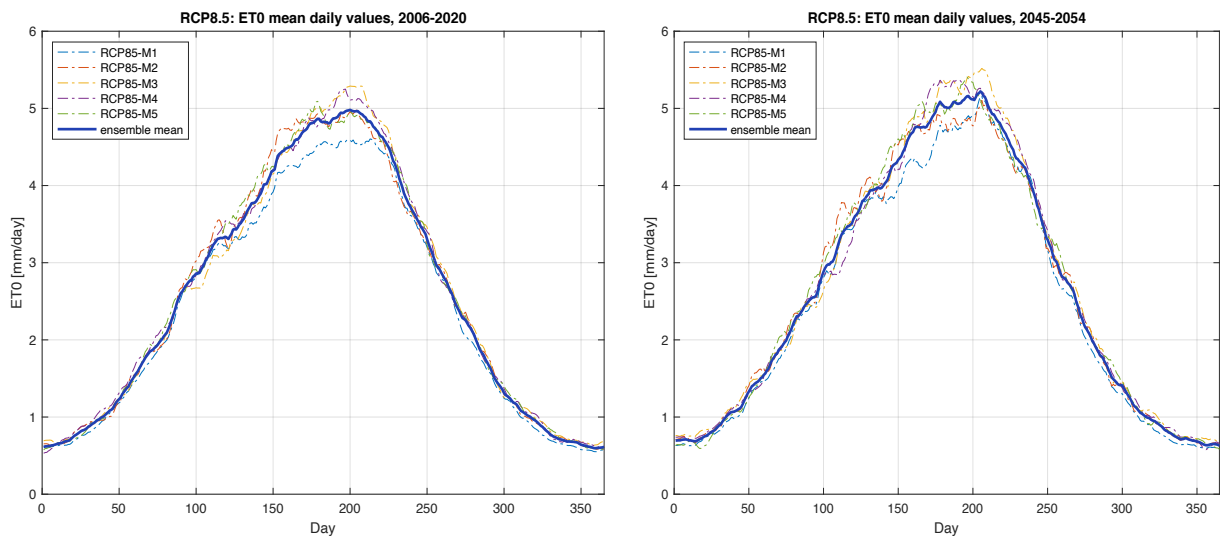


Figure 3.13: Reference evapotranspiration annual behaviour for the present period (2006-2020, left) and the future decade 2045-2054 (right), RCP8.5 scenario.

Summer is the season which shows the highest variability between the climate datasets used. Figure 3.15 represents in detail the situation with box plots for the summer total ET_0 (June, July, and August) from 2006 to 2055. It is possible to observe the high inter-annual variability of the series and the different distributions of values which characterize each dataset. This variability is higher for the scenario RCP8.5, with each dataset having a larger range of values over the 50 years compared to RCP2.6. Even though the median value is different from dataset

to dataset, it increases from RCP2.6 to RCP8.5 for all of them. In the next chapter the results of the crop modelling will be discussed, and it will be important to remember that those results come from datasets with this degree of variability.

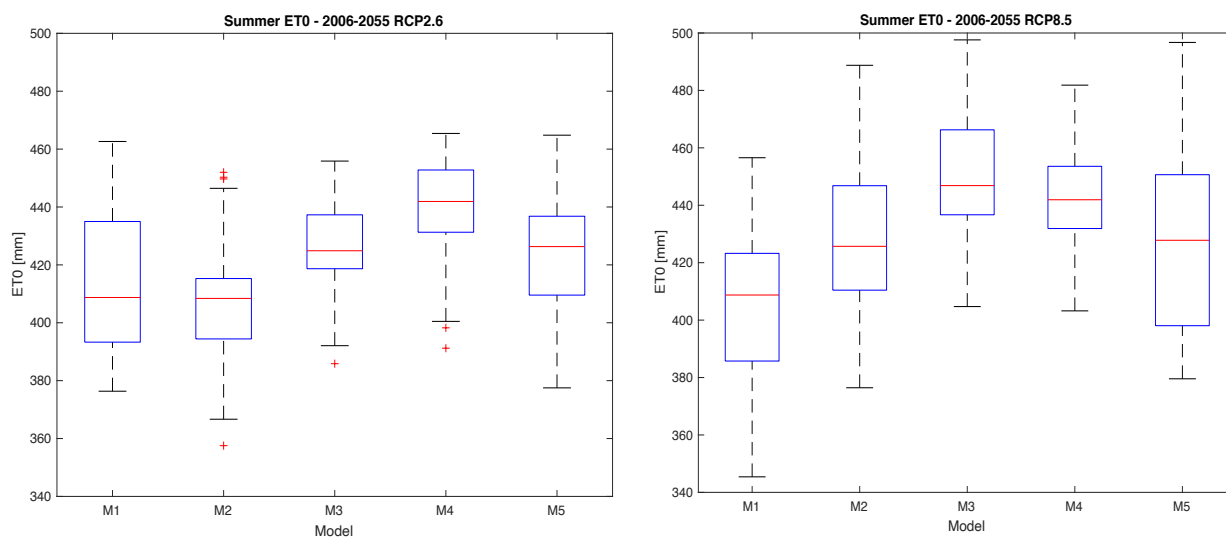


Figure 3.15: Boxplots over 2006-2055 for summer (June, July, August) total ET_0 relative to each climate model.

Chapter 4 Crop model results

The hydrological model presented in Chapter 1 was applied to estimate daily timeseries of ET_c , ET_a , ET_{green} , water stress coefficient k_s , and irrigation requirements $IrrReq$ for maize at the local study site for the *present* (2006-2020) and the future period 2021-2055.

In this chapter, the results obtained for both RCP2.6 and RCP8.5 are presented and discussed. The crop model results coming from the five different climate model couples' datasets were averaged in order to minimize the biases and errors of each single model. These averaged values will be referred to from now on as *ensemble results* or *ensemble mean*. The future period has been subdivided into three sub-periods to help the study of the future evolution of the variables: *2030* (2025-2034), *2040* (2035-2044), *2050* (2045-2054).

Other interesting considerations came from the computation of some indices such as the crop water requirement (CWR), number of irrigation days and precipitation days. To calculate the future trends of those indices, as well as future trends of the five main variables, totals for each future year were calculated and the timeseries were plotted together with their trends over the whole period.

At the end of the chapter the results related to two possible agricultural adaptation strategies are also presented.

4.1 *Present* results

Here the results from the modeling of the *present* period 2006-2020 are briefly presented to have a meter of comparison for the discussion of the future projections. In Figure 4.1 the main outputs for the rainfed (left) and irrigated (right) conditions are shown for the ensemble mean. The daily average over the 15-years period 2006-2020 is depicted. The situation related to the two RCPs do not differ much, with similar behavior of ET_a , ET_c and ET_{green} for the two climate scenarios.

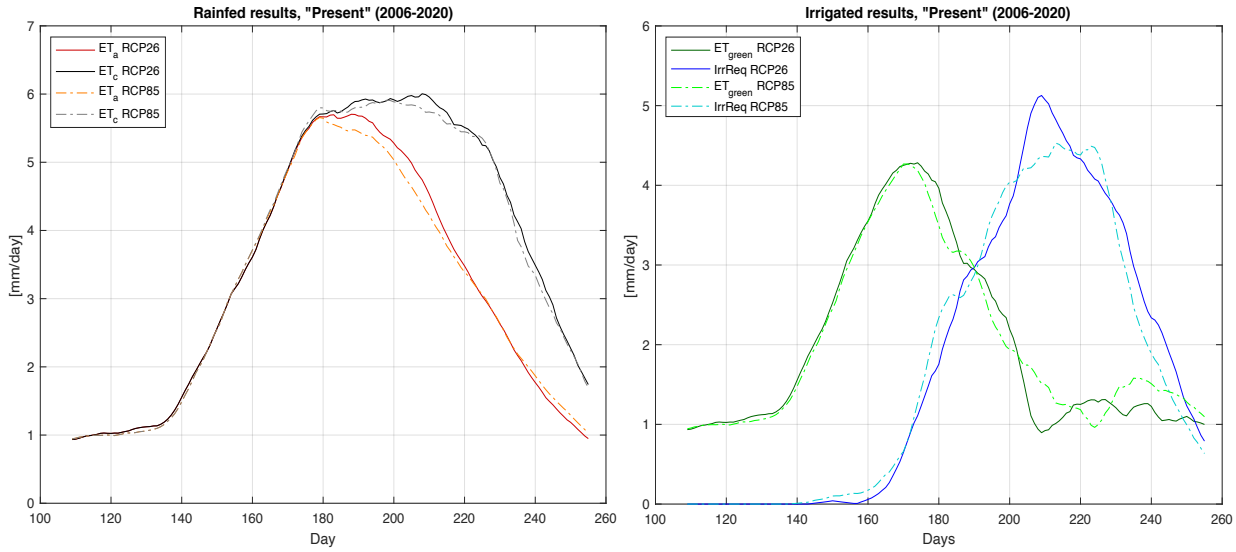


Figure 4.1: Results of the modeling for the rainfed and irrigated cases, represented respectively by the average year values for ET_a and ET_c (left) and for ET_{green} and $IrrReq$ (right), present period.

On the other hand, the irrigation requirements $IrrReq$ of the two RCPs seem to be quite different, but if the mean of the annual irrigation requirements and the number of irrigation days are considered the distance between the two cases is relatively small (Table 4.1). In Table 4.1 the mean values of these two variables are shown together with the standard deviation over the 15-years period, to represent the inter-annual variability of the results. An irrigation day is a day for which the irrigation requirements are more than 2 mm. The irrigation requirement represents the difference between the crop water requirement and effective precipitation (ET_{green}). As explained in Chapter 1, the modeling for $IrrReq$ was performed considering the minimum water amount needed to avoid water stress completely (k_s always equal to 1).

Table 4.1: Mean and standard deviation of annual irrigation requirements and number of irrigation days (irrigated case) over the period 2006-2020, both RCP2.6 and RCP8.5.

	<i>Annual IrrReq (mm/year)</i>		<i>Number of irrigation days</i>	
	Mean	SD	Mean	SD
RCP2.6	262.47	43.67	58	11
RCP8.5	256.25	63.82	55	12

The plot in Figure 4.1 shows the contextual increase of $IrrReq$ with the decrease of ET_{green} , which happens as spring comes to an end and precipitations start being scarce. The date on which the water stress starts, considering the average over the *present* period, is at the end of spring, the 164th day of the year under RCP2.6 conditions (13th of June), and the 158th day of

the year for RCP8.5 (7th of June). The first day of the year for which k_s is less than 1 have been considered as the start of water stress.

Table 4.2 shows mean and standard deviation over the period 2006-2020 of parameters characterizing the rainfed case (no irrigation): number of water stress days, crop water requirement, and cumulative ET_a . A water stress day is a day for which k_s is less than 1. The crop water requirement CWR represents the water that needs to be supplied to avoid water stress over the whole growing period. In other words, it is the water required to compensate the evapotranspiration loss from the cropped field (Allen et al, 1998), and in this work it is calculated as the sum of all the daily values of ET_c over the growing period of n days:

$$CWR = \sum_{i=1}^n ET_c \quad (4.1)$$

where n is equal to 153 days in the case of maize growing season (from the 16th of April to the 15th of September). It is useful to compare the CWR to the annual cumulative ET_a (sum of all ET_a daily values over the growing period), to have an indication of how much water is missing from an optimal development of the crop. The crop suffers from water stress if not irrigated. This is demonstrated by the number of water stress days being almost the 50% of the total 153 days of maize growing season, and by the cumulative ET_a being less than the CWR .

Table 4.2: Mean and standard deviation of CWR , cumulative ET_a , and number of water stress days (rainfed case) over the period 2006-2020, both RCP2.6 and RCP8.5. Between brackets the fraction of stress days over the total of the growing season.

	<i>Number of water stress days</i>		<i>CWR (mm/year)</i>		<i>Cumulative ET_a (mm/year)</i>	
	Mean	SD	Mean	SD	Mean	SD
RCP2.6	71 (46%)	10	557.92	10.35	461.29	23.10
RCP8.5	75 (49%)	11	553.58	16.47	454.12	33.81

The results for the annual irrigation requirements shown in Figure 4.1 are coherent with the real data, since for the agricultural season 2009-2010 in the area studied the water used for irrigation of maize fields was around 251 mm/year (ISTAT, 2010), and the model projected $IrrReq$ is in the same order of magnitude. Furthermore, as explained previously, it appears clear that maize needs to be irrigated at the latitude of study to secure a proper production, and this is again coherent with the actual situation in the area, which sees maize being the most important irrigated crop for fraction of irrigated hectares (ISTAT, 2010).

4.2 Future projections

After the analysis of the *present* results, the focus will go over to the future projections.

4.2.1 Crop water requirements and actual evapotranspiration

Firstly, the rainfed case is briefly analyzed to understand which effects the projected climate trends of the two RCPs may have on maize growth independently from the irrigation provided. Figure 4.2 illustrates the comparison between the two RCP scenarios of daily actual evapotranspiration (daily series obtained averaging the daily values over the whole 35 years period 2021-2055). The results for RCP8.5 show an earlier peak in ET_a and a steeper decrease than RCP2.6. The steeper decrease of ET_a could be seen as indication of higher water stress during the last growing phase of maize since the value of ET_a depends directly on the water stress coefficient k_s . In Figure 4.2 the ensemble mean is shown together with the series obtained from each climate model, to represent the uncertainty degree of the future projections.

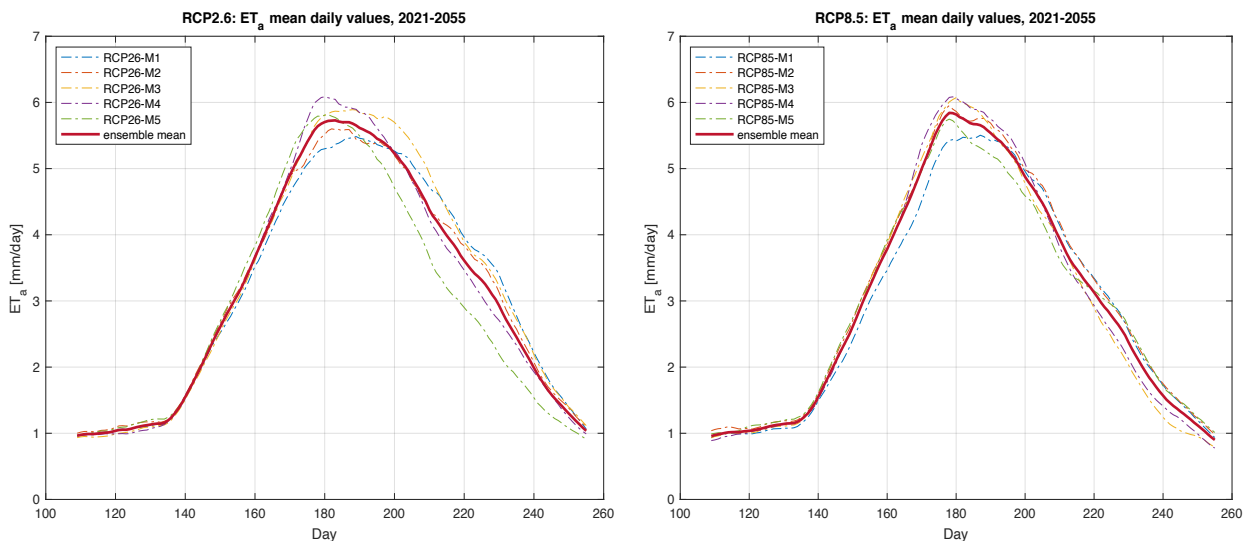


Figure 4.2: ET_a average year over the 35-years period 2021-2055, for RCP2.6 (left) and RCP8.5 (right). Each model is shown together with the ensemble mean.

To analyze further the situation, Table 4.3 reports the annual CWR and cumulative ET_a for the three future decades. Only the ensemble mean values are represented for the sake of simplicity, but it is important to remember that all the values are an average of the different outputs from

the five climate datasets used, as depicted in Figure 4.2 for ET_a . The cumulative ET_a is always lower than CWR , showing how without irrigation the crop would always be in water stress over the whole future period.

Table 4.3: Average values of CWR and cumulative ET_a for the future decades 2030,2040,2050 (RCP2.6 and RCP8.5)

	<i>CWR (mm/year)</i>		<i>Cumulative ET_a</i>	
	RCP2.6	RCP8.5	RCP2.6	RCP8.5
2030	550.87	555.86	464.36	440.62
2040	543.28	555.43	459.89	448.65
2050	545.36	565.30	465.52	440.77

Figure 4.3 shows the trend of CWR from 2021 to 2055 (ensemble mean). The inter-annual variability is high, but it is still possible to appreciate the increasing trend projected by RCP8.5 and the differences between the two scenarios, especially over the decade 2045-2054. The higher CWR values of RCP8.5 compared to RCP2.6 come probably from the projected rise of temperatures under RCP8.5 conditions, as presented in Chapter 3.

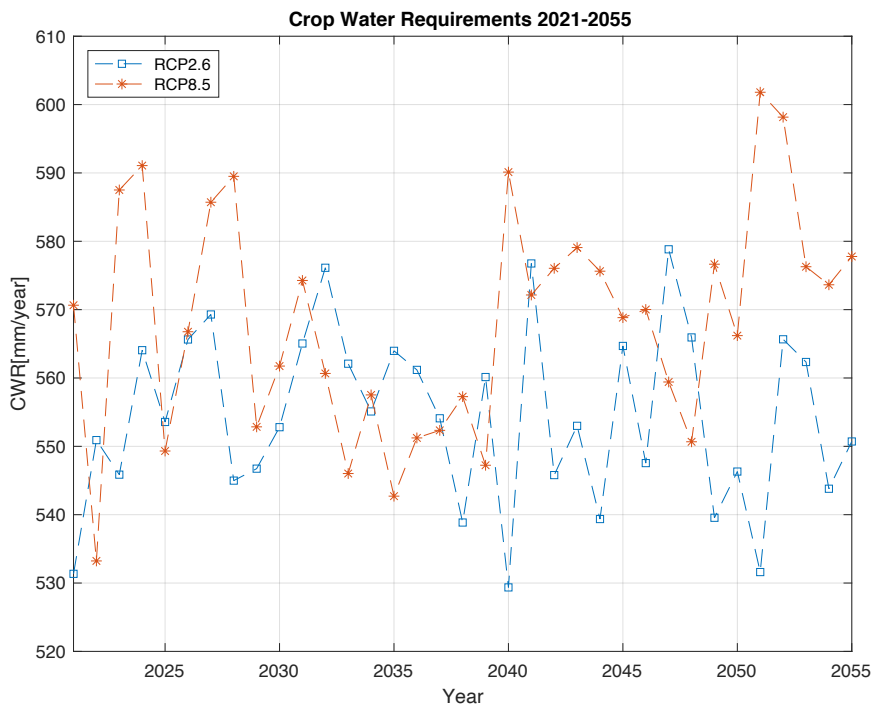


Figure 4.3: Crop water requirement series from 2021 to 2055

4.2.2 Water stress

The plant is in water stress condition when it does not have enough water to sustain its growth (i.e., when the available water in the soil is less than the crop evapotranspiration for that day). One interesting thing to analyze is which day the water stress starts on in the two scenarios. Does this date change through the years? Does climate change have a role in this change?

Before analyzing this feature though, it is necessary to point out that water stress in rainfed and irrigated scenarios starts in different dates. This comes from how the model calculates k_s (water stress coefficient). k_s depends on the rooting depth, and so on the amount of available water for the plants' growth. The maximum rooting depth in rainfed conditions is considered longer than for irrigation assumption because the plants invest more energy to be able to reach the water they need while with irrigation they have no stimulus in doing so. In this work the focus was only on the water stress in rainfed scenario to answer the question, what will happen if irrigation is not present or not sufficient?

In Table 4.4 the water stress dates cited before are shown for the ensemble mean (rainfed case). The water stress starts later in the future for RCP2.6, probably due to the optimistic climate assumptions of this scenario, meanwhile for RCP8.5 there is not a clear trend, since in 2040 the stress starts later than 2030 and 2050. This could be due to a loss of detail on the inter-annual variability caused by the averaging performed over the decades.

Table 4.4: Start of water stress days

RCP2.6			RCP8.5		
2030	2040	2050	2030	2040	2050
19 th of June	21 st of June	29 th of June	13 th of June	19 th of June	15 th of June

It could be useful then to analyze further the water stress during the growing season, looking at the number of stress days in a year (a water stress day is a day for which k_s is less than 1) for the rainfed scenario. Table 4.5 depicts the total number of stress days over the growing season (from the 16th of April to the 15th of September, a total of 153 days) for the three future decades (ensemble mean). The mean values for each decade are shown together with the standard deviation SD over the 10-years period. Maize results to be in water stress for half its period of

growth in almost all the cases. The situation is quite similar between the two climate scenarios, considering also that the delta between the respective RCPs values of each decade is less than the standard deviation.

Table 4.5: Mean values and standard deviations of water stress days in a year over each decade, and percentage over the total days of the growing season.

	RCP2.6			RCP8.5		
	Mean	SD	Season %	Mean	SD	Season %
2030	77	9	50%	76	14	50%
2040	75	7	49%	76	11	50%
2050	71	7	46%	78	9	51%

So far, it seems that water stress is not affected much by the climate, since there is a similar situation between RCP2.6 and RCP8.5 future projections. But another step of the analysis needs to be made, since the volume of water deficit does not depend only on the number of stress days, but also on the gravity of that stress (i.e., how much k_s is less than 1). The smaller k_s , the higher the stress for the crop is. Figure 4.4 shows the histograms of k_s values for the *present* period and the furthest future decade (2050). Looking at these graphs, it is important to remember that the total number of k_s values is 153, one daily value for each day of maize growing season from April to September. Firstly, it is possible to see that the stress under RCP8.5 for the *present* period is not as severe as in the projected conditions. In the 2050 decade indeed, the frequency distribution of k_s is shifted towards lower values, with values in the [0.40-0.50] bin, while the lowest values for the *present* are in the [0.50-0.60] bin (Figure 4.4). The situation is the opposite of RCP2.6, for which the period 2006-2020 is the one with the lowest values of stress coefficient.

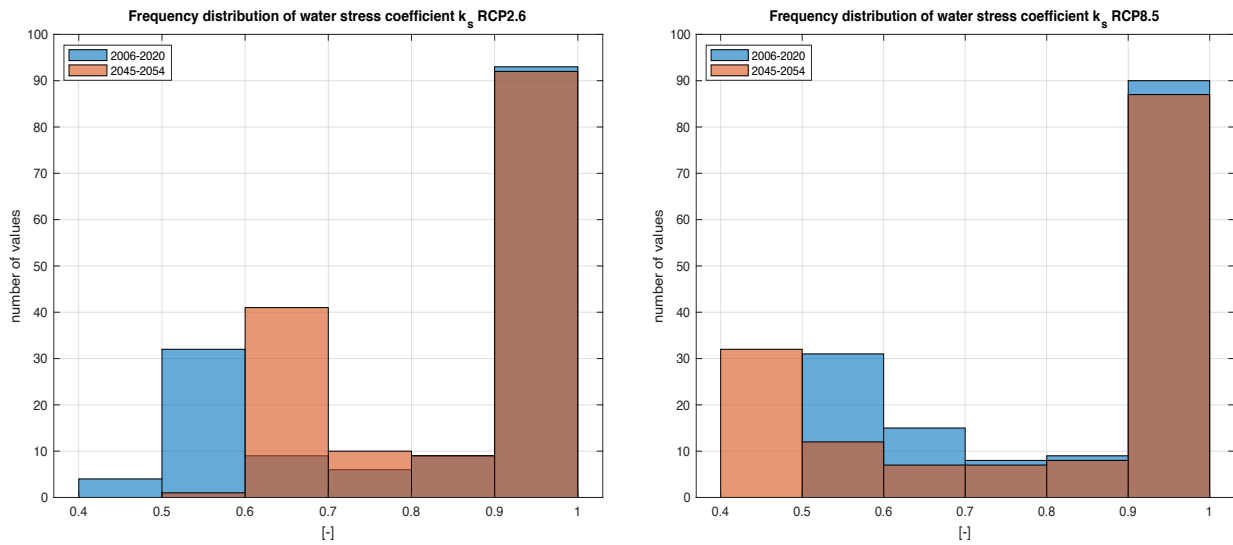


Figure 4.4: Frequency distribution of k_s values and comparison between the present period and 2050, for both RCP2.6 (left) and RCP8.5 (right).

It has been said that water stress starts in June, but also that it is important to consider the gravity of the water stress. To assess when the water stress is more severe over the whole growing season, the monthly distribution of severe water stress days (days for which k_s is less than 0.6) has been plotted in Figure 4.5. The bar graph shows the detail for each month of maize growing period, considering k_s values for the average year of each decade. The values for the *present* period have been plotted too for comparison (for each of the four periods the mean daily values were calculated averaging for each day over the 15- or 10-years period). August and September seem to be the most critical months for maize development, being the only two months in which the stress coefficient reaches values smaller than 0.6. The situation in the two RCPs is very different. RCP2.6 is very optimistic projecting a decrease of water stress days in the future, while RCP8.5 projects an increase of the stress. The studies performed by Arpa Piemonte on both historical and future series of temperature and precipitation of the region Piemonte found that summer will see a gradual decrease of rainfalls, and the first district experiencing that will be Cuneo (Arpa Piemonte, 2020a), the district that is being analyzed in this work. This could suggest that even though it was made the choice of studying the most “optimistic” and the most “pessimistic” climate scenarios to represent the complete range of possibilities for the future, the projections by RCP2.6 might be too optimistic and RCP8.5 projections seem more in line with the other future projections in literature (Arpa Piemonte, 2020a).

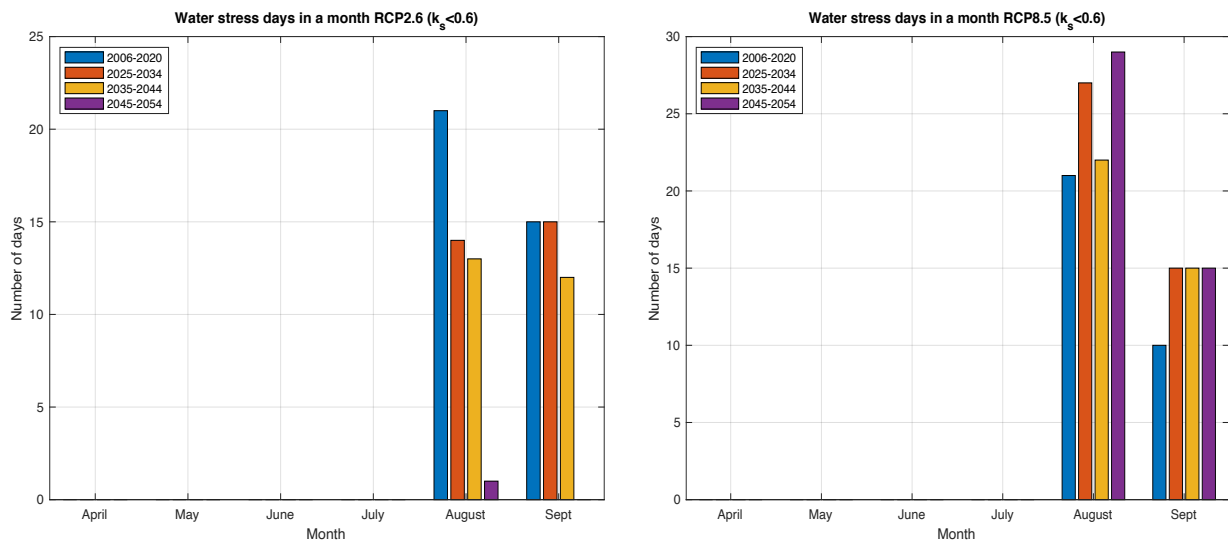


Figure 4.5: Number of severe water stress days ($k_s < 0.6$) for each month, RCP2.6 (left) and RCP8.5 (right).

All these considerations lead to the conclusion that at the latitude of study, maize needs to be irrigated, since already in the *present* period the plant in rainfed conditions would suffer of water stress for almost half of its growing season, and that in the future the situation could worsen, especially considering RCP8.5 assumptions. These findings are coherent with the current reality of the area, where maize is the first irrigated crop per number of hectares irrigated, as illustrated already in Chapter 3.

4.2.3 Irrigation requirements

In the previous section, it has been said that in the latitude of study, irrigation is necessary to grow maize properly. The next questions to answer then are how will irrigation requirements change in the future? What will the difference be considering two different climate projections (RCPs)?

Firstly, the variable irrigation requirement *IrrReq* is demonstrated to be sensitive to climate change. In Figure 4.6 the mean values for the *present* (2010 on the plot), and future decades 2030, 2040, 2050 are shown, where the lines represent the ensemble mean values while the shades represent the range of ± 1 standard deviation between the five different climate model projections used. The variability between the climate datasets is high, probably due to the differences in predicted precipitations and ET_0 shown in Chapter 3. However, the *IrrReq*

increasing trend projected under RCP8.5 is clear, with an average increment of 16% by 2050 compared to the *present* value. This increment is mainly due to the reduction of total summer precipitations and the rise of summer temperatures characterizing the climate scenario. On the other hand, RCP2.6 assumptions cause a *IrrReq* reduction on average of 13% by 2050, and even considering the shaded range there is not an increase of *IrrReq* as important as RCP8.5.

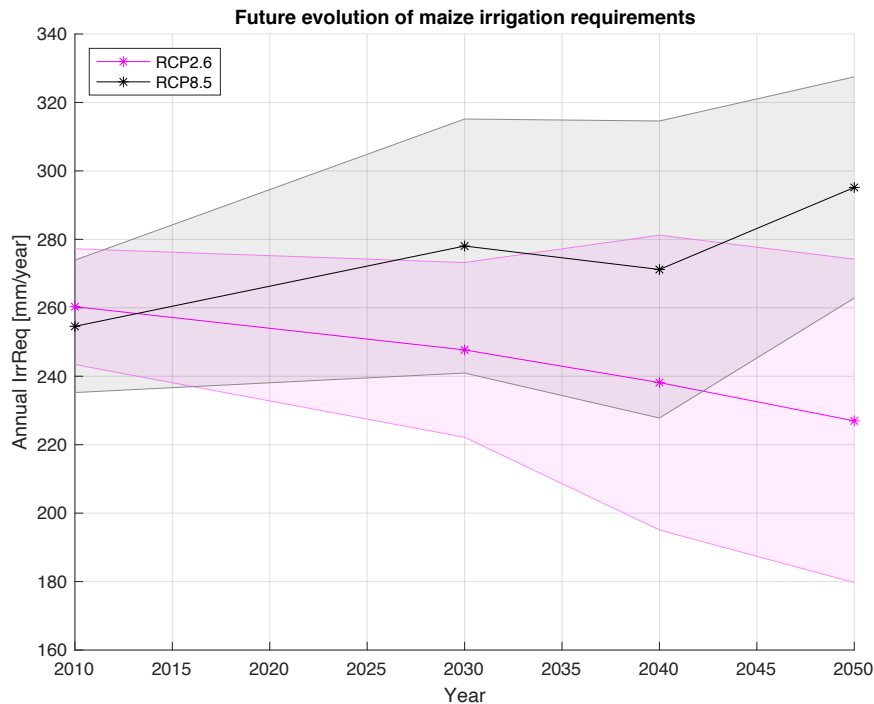


Figure 4.6: Evolution of *IrrReq*, considering the average values over the four periods present (2006-2020), 2030 (2025-2034), 2040 (2035-2044), 2050 (2045-2055). Two RCPs and shaded range (Campbell, 2022) for standard deviation between the five climate datasets.

Figure 4.7 depicts the detail of 2050 daily irrigation requirements, for the ensemble mean and each of the models. As seen in the previous plot, the inter-model variability is high, but the higher peak of *IrrReq* under RCP8.5 hypotheses compared to the RCP2.6 situation is evident for all the models and the ensemble mean. Irrigation starts to be needed at the beginning of June and the peak of daily *IrrReq* happens on average in August.

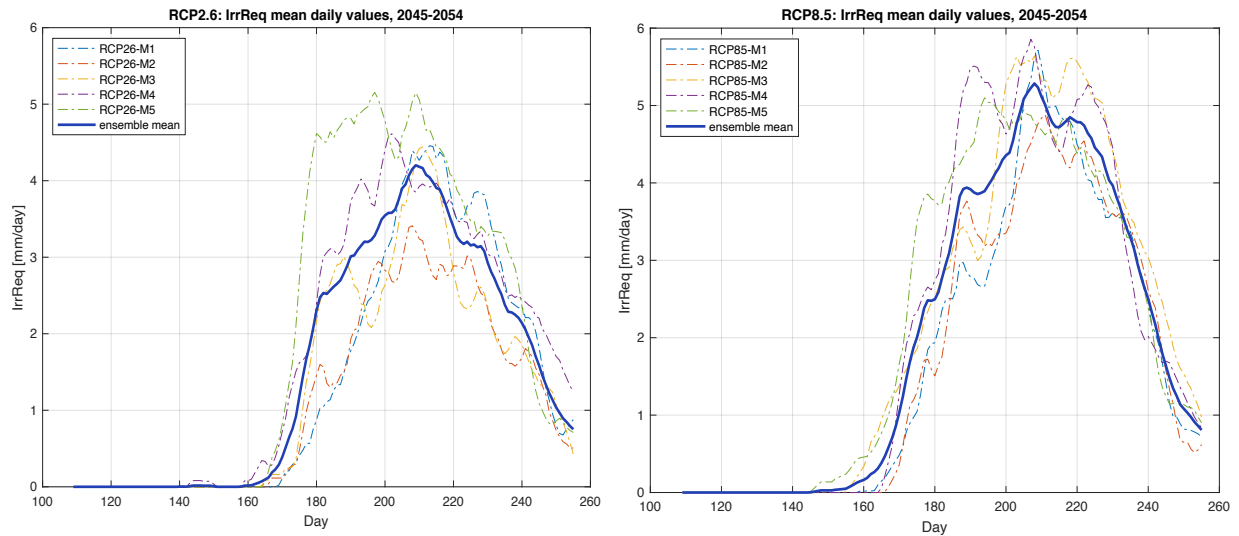


Figure 4.7: Irrigation requirements mean annual behavior during 2045-2054, for the two climate scenarios RCP2.6 (left) and RCP8.5 (right).

The inter-annual variability is another important aspect to be analyzed. The box plots in Figure 4.8 summarizes the situation. M1 shows the highest temporal variability for RCP2.6, while M5 has this role in RCP8.5. All the models show higher values on average under RCP8.5 than RCP2.6.

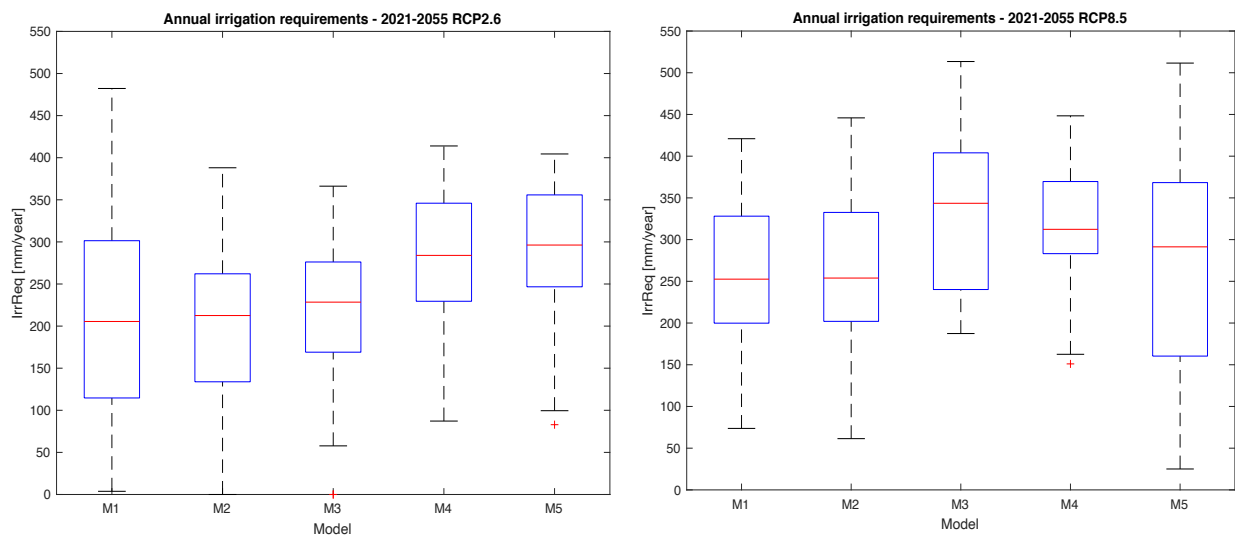


Figure 4.8: Boxplots over 2021-2055 for annual irrigation requirements relative to each climate dataset, RCP2.6 (left) and RCP8.5 (right).

Lastly, to better understand the situation, the annual number of irrigation days and the number of precipitation days have been computed and the trends for these two variables from 2006 to 2055 for both the RCP scenarios are shown in Figure 4.9. An irrigation day ID is a day for which the irrigation requirement is higher than 2 mm/day. A precipitation day PD is a day for which precipitations are higher than 2 mm/day. Irrigation days are always higher in number than precipitation days, and this is coherent with the results of previous literature for this climate area, Sub-Continental Temperate (Rolle et al., 2022). The trend of ID decreases for RCP2.6, while it increases for RCP8.5. The rise of RCP8.5 irrigation days matches the decrease in precipitation days, even though the trend of PD is less evident. More ID often signifies bigger volumes of irrigation requirements, because this volume results from a larger number of stress events (Rolle et al., 2022). These findings are coherent with the studies performed by Arpa Piemonte on both historical and future series of temperature and precipitation of the region, which found for RCP8.5 a decreasing trend in precipitation days from 2011 to 2100, as well as a length increase of dry periods (Arpa Piemonte, 2020a).

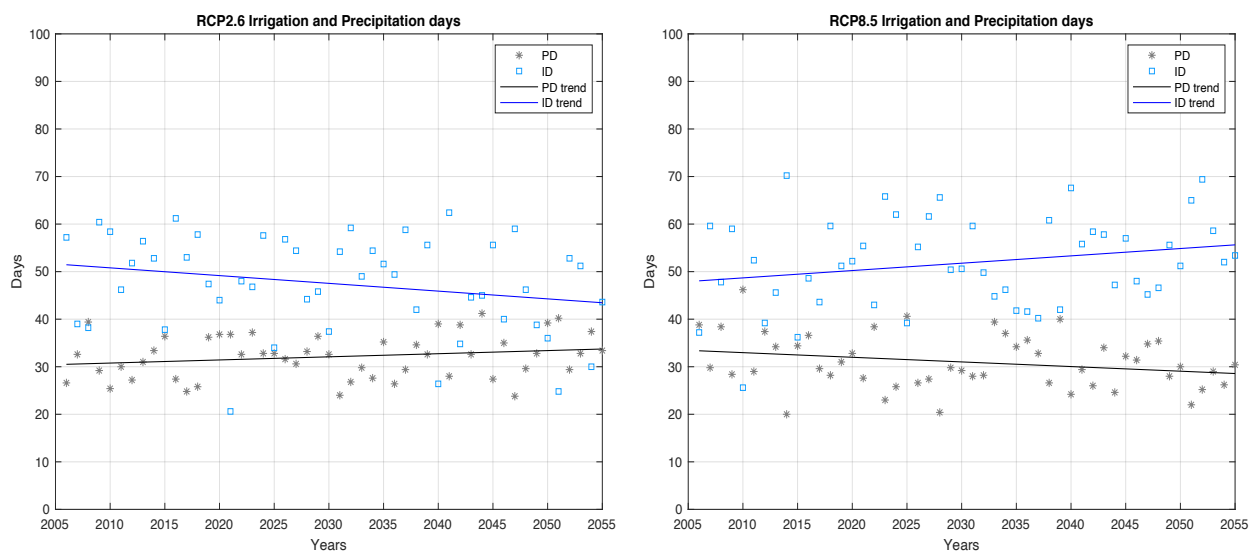


Figure 4.9: Trend of total annual irrigation days and precipitation days from 2006 to 2055, RCP2.6 (left) and RCP8.5 (right).

4.3 Crop adaptation, early sowing

It has been just presented how in the future the irrigation requirements of maize are projected to increase under pessimistic climate change assumptions (RCP8.5). Moreover, trends in historical series of observations in the region over the last 60 years (1958-2018) already show a reduction of 13% of the winter precipitations and an increment of the daily maximum temperatures of 2°C (Arpa Piemonte, 2020b). In this context, it can be useful to analyze some possible adaption strategies to help facing the challenges that climate change brings over the maize production and the agricultural production in general of the area studied. With adaptation strategies it is meant all the responses to actual or projected climate change effects that moderate its harms and exploit its beneficial opportunities. Examples of adaptation strategies for agriculture are improving irrigation efficiency, changing the cropping pattern and calendar of planting, planting of drought resistant varieties of crops, etc.

The first adaptation strategy that has been analyzed in this work is to anticipate the sowing and harvesting dates, in order to have the developing phase of the plant and the flowering in June, with the maximum solar radiation and more water available. Harvesting earlier should also allow to use less irrigation water in summer, avoiding the worst months for water availability (August and September). Two experiments were performed to study the effects of this strategy on crop irrigation requirements: anticipating of 15 days and of 31 days the sowing and harvesting of maize. The length of the growing period was kept constant at 153 days. Table 4.6 shows the dates of sowing and harvesting for the three runs of the model (experiments).

Table 4.6: Anticipated sowing and harvesting dates compared to the originals, in brackets there are the progressive number for the specific day in a year (from 0 to 365)

Experiment	Sowing	Harvesting
Original	16 th of April (106)	15 th of September (258)
15 days	1 st of April (91)	31 st of August (243)
31 days	16 th of March (75)	15 th of August (227)

To analyze this strategy with the crop model used in this study it is sufficient to change the original sowing and harvesting dates given as inputs to the crop model to the dates shown in Table 4.6 (15 days and 31 days). None of the other inputs were changed to perform these new runs of the crop model.

It is necessary to note though, that in this analysis impacts on the yield due to lower temperatures and radiations are not taken into account. The risk of this strategy is indeed of frosts in late spring that could drastically reduce the production. It was not possible to analyze further this aspect in this work, since the focus of the study was on irrigation requirements.

Lastly, all the results presented refer to the ensemble mean, to being able to focus more on the temporal variability and on the comparison with the original situation.

4.3.1 Crop water requirements and water stress

The aim of studying this adaptation strategy in this work is to assess its effects on maize irrigation requirements, so the analysis will focus more on those results than the results about actual evapotranspiration and water stress. A short overview of the results about these two variables for the rainfed case is here presented to give more context to *IrrReq* analysis.

Figure 4.10 and Figure 4.11 show the comparison of crop water requirements (*CWR*) series from 2021 to 2055 between the three sowing dates, for RCP2.6 and RCP8.5 respectively. The inter-annual variability of the “anticipated” series is the same of the series for the original sowing date. The influence of the climate scenarios on this variable is clear with peaks of *CWR* over 600 mm/year under RCP8.5 hypothesis (Figure 4.11), while it reaches barely over 580 mm/year considering RCP2.6 assumptions (Figure 4.10). It seems that from the point of view of *CWR* alone, anticipating the sowing date of 15 days (1st of April) does not make a relevant difference, while sowing on the 16th of March visibly reduces the *CWR*.

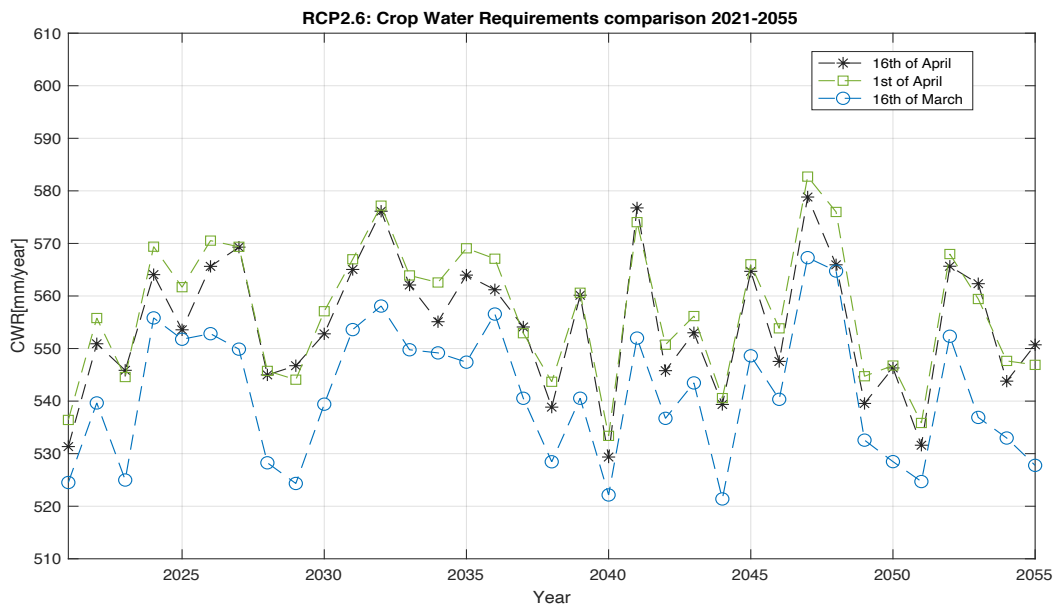


Figure 4.10: Annual series of crop water requirements 2021-2055 under RCP2.6, comparison between the three sowing dates.

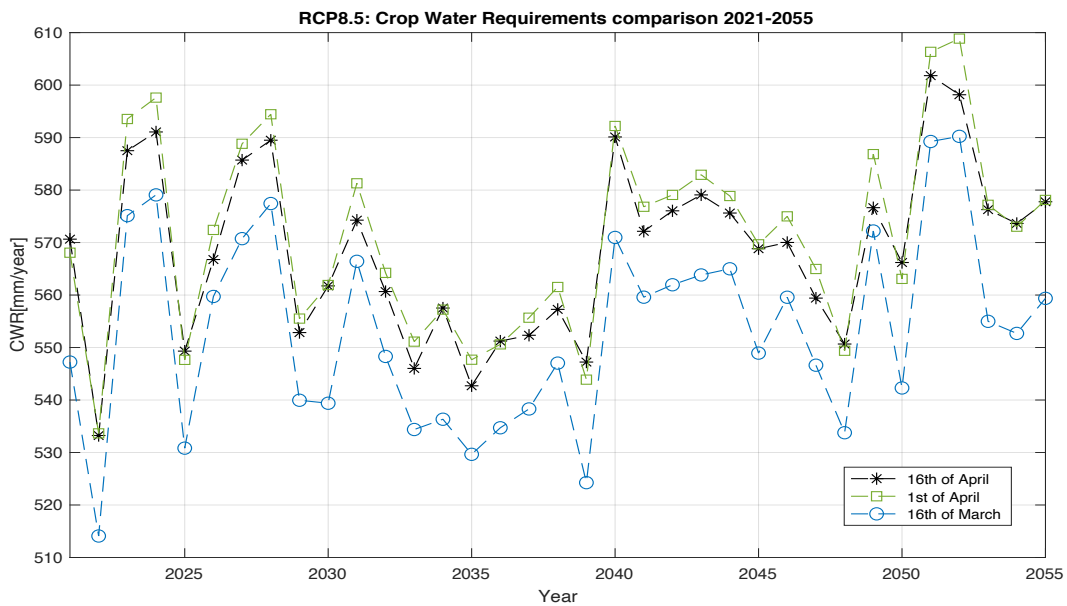


Figure 4.11: Annual series of crop water requirements 2021-2055 under RCP8.5, comparison between the three sowing dates.

The number of monthly water stress days is briefly examined here, similarly to the analysis carried out in the previous chapter. Table 4.7 collects the percentage variations of number of severe water stress days from the number of the original sowing date (16th of April) of the respective scenario and decade. A severe water stress day is a day for which k_s is less than 0.6. The results meet the expectations for this adaptation strategy, with the number of water stress

days reducing as the growing season is anticipated. In the case of the 1st of April there are already some positive effects on the stress, but the biggest reduction happens with the sowing on the 16th of March, which brings the days of stress to zero in RCP2.6 case (a reduction of 100%).

Table 4.7: Number of severe water stress days ($k_s < 0.6$) for the sowing dates April 1st and March 16th.

	1 st of April		16 th of March	
	RCP2.6	RCP8.5	RCP2.6	RCP8.5
2030	-45%	-21%	-100%	-50%
2040	-56%	-14%	-100%	-41%
2050	+400%	-18%	-100%	-45%

A more detailed monthly representation of these values is depicted in Figure 4.12 and Figure 4.13, for RCP2.6 and RCP8.5 respectively. In these plots the mean monthly values for each decade are depicted. Only the months from June to September are shown since they are the only months in which water stress happens. The values relative to the original sowing date are also reported, in order to understand better the meaning of the percentages shown in Table 4.7. August is confirmed to be the most critical month in terms of water stress for all the scenarios. The positive effects of the early sowing are due to the fact that it allows to harvest earlier and so to avoid the days on which water scarcity is greater. For example, sowing on the 16th of March leads to harvest on the 15th of August, shifting most of the growing season to June and July during which the water availability is higher.

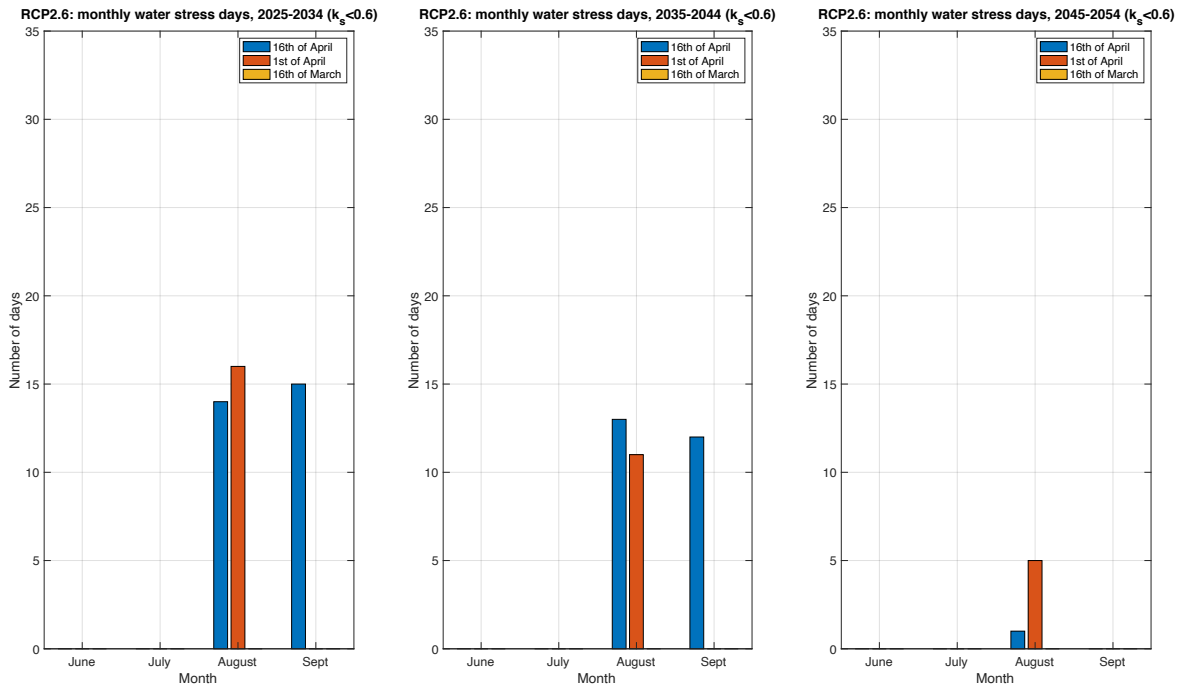


Figure 4.12: Comparison between the number of severe water stress days ($k_s < 0.6$) relative to the three different sowing dates, for the three future decades (RCP2.6).

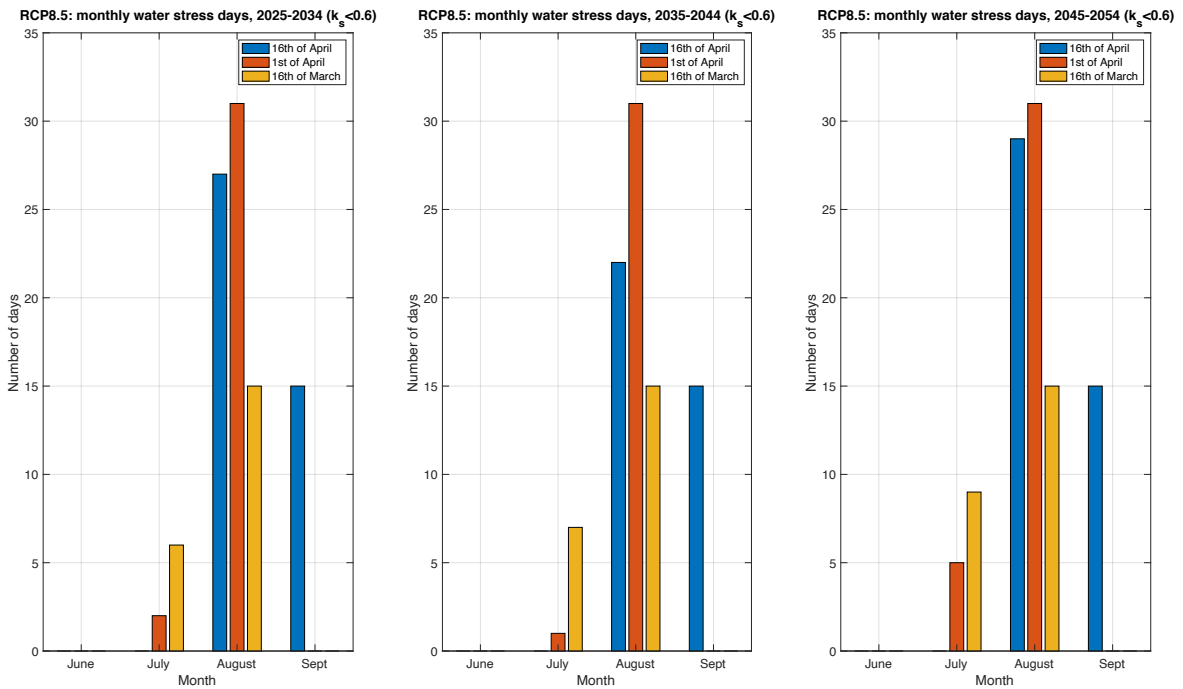


Figure 4.13: Comparison between the number of important water stress days ($k_s < 0.6$) relative to the three different sowing dates, for the three future decades (RCP8.5).

4.3.2 Irrigation requirements

Now the changes in irrigation requirements due to the different sowing dates will be analyzed in detail, to evaluate if this could be a useful adaptation strategy (i.e., if it may reduce the future irrigation requirements).

The plots in Figure 4.14 represent the average over the 35-years future period (2021-2055) of the daily timeseries of irrigation requirements $IrrReq$ and ET_{green} . It is possible to appreciate the difference on the behavior of these two variables made by the anticipated sowing dates. The earlier start of the growing season and the shift of the peaks of the curves of the two variables appear clearly in these two plots. The reduction of $IrrReq$ and the increase of ET_{green} are particularly evident for the sowing on the 16th of March. This happens thanks to the more present precipitations in late spring/early summer compared to the water scarcity typical of August and early September.

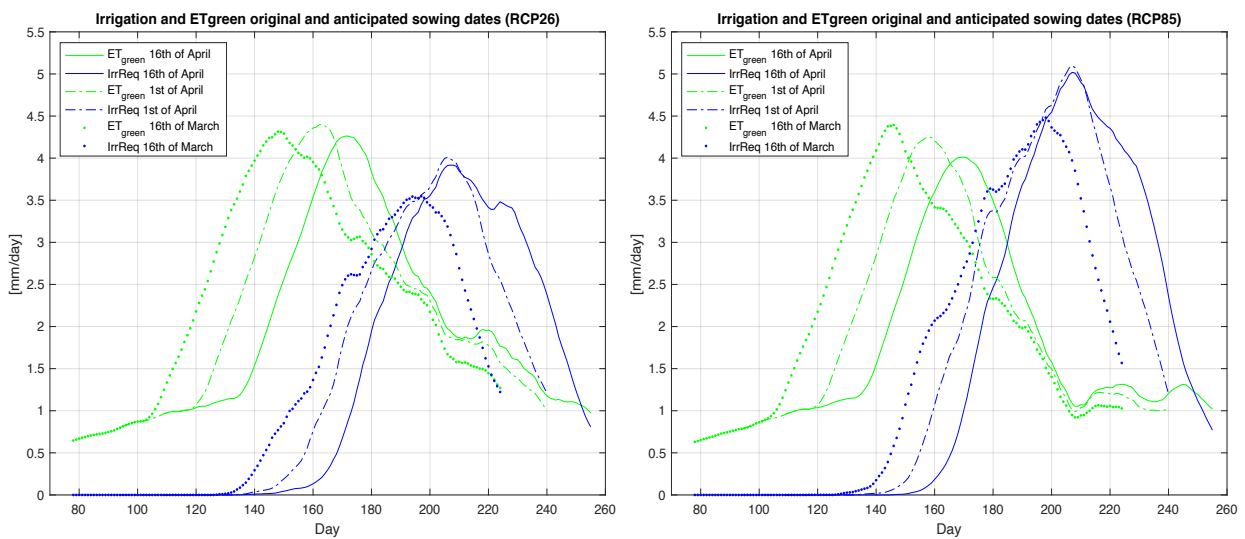


Figure 4.14: Comparison of $IrrReq$ and ET_{green} annual distribution of daily values for the three different planting dates. The comparison is plotted for RCP2.6 (left) and RCP8.5 (right).

One way to have a quantitative information of how much anticipating the sowing date could help is looking at the total annual $IrrReq$ and at the number of irrigation days in a season. These values are collected in Table 4.8 and Table 4.9 together with the percentage variations from the respective decade and scenario relative to the original sowing date (between brackets). Anticipating the sowing date is projected to reduce irrigation requirements by 2050, with an

ensemble average from -3% to -16% compared to 2050 of original date, depending on climate scenario and sowing date.

Table 4.8: Mean values of annual irrigation requirements (mm/year) over each of the three future decades for the sowing dates April 1st and March 16th (RCP2.6 and RCP8.5). In brackets the percentual variations.

(mm/year)	1 st of April		16 th of March	
	RCP2.6	RCP8.5	RCP2.6	RCP8.5
2030	231.20 (-8%)	271.09 (-3%)	200.61 (-20%)	236.52 (-15%)
2040	221.25 (-8%)	260.04 (-5%)	188.52 (-23%)	227.62 (-17%)
2050	220.61 (-4%)	287.54 (-3%)	198.67 (-13%)	249.30 (-16%)

Table 4.9: Mean annual number of irrigation days ID (-) over each of the three future decades for the sowing dates April 1st and March 16th (RCP2.6 and RCP8.5). In brackets the percentual variation.

(-)	1 st of April		16 th of March	
	RCP2.6	RCP8.5	RCP2.6	RCP8.5
2030	62 (-6%)	65 (+3%)	48 (-27%)	60 (-5%)
2040	54 (-5%)	62 (-3%)	50 (-12%)	51 (-20%)
2050	57 (-10%)	68 (0%)	53 (-16%)	66 (-3%)

The bar plot in Figure 4.15 allows to visually assess the difference in annual *IrrReq* between the three sowing dates, keeping always in mind the inter-annual variability of this variable, represented in the plot by the standard deviation bars. In Figure 4.15 it is also possible to appreciate the difference made on the projected results by the two climate hypotheses. For RCP2.6 the irrigation requirements decrease through the studied period, for all the three sowing dates considered, consistently with the decreasing trend of irrigation days and increasing of precipitation days presented in the previous paragraph (4.2.3). On the other hand, RCP8.5 projects an increase of *IrrReq* through the decades for all the sowing dates, and this is consistent with the decrease of precipitation and the higher temperature characterizing this scenario. As illustrated in Chapter 3, RCP8.5 projects a raise in summer temperatures and a decrease in summer precipitations from 2006 to 2055.

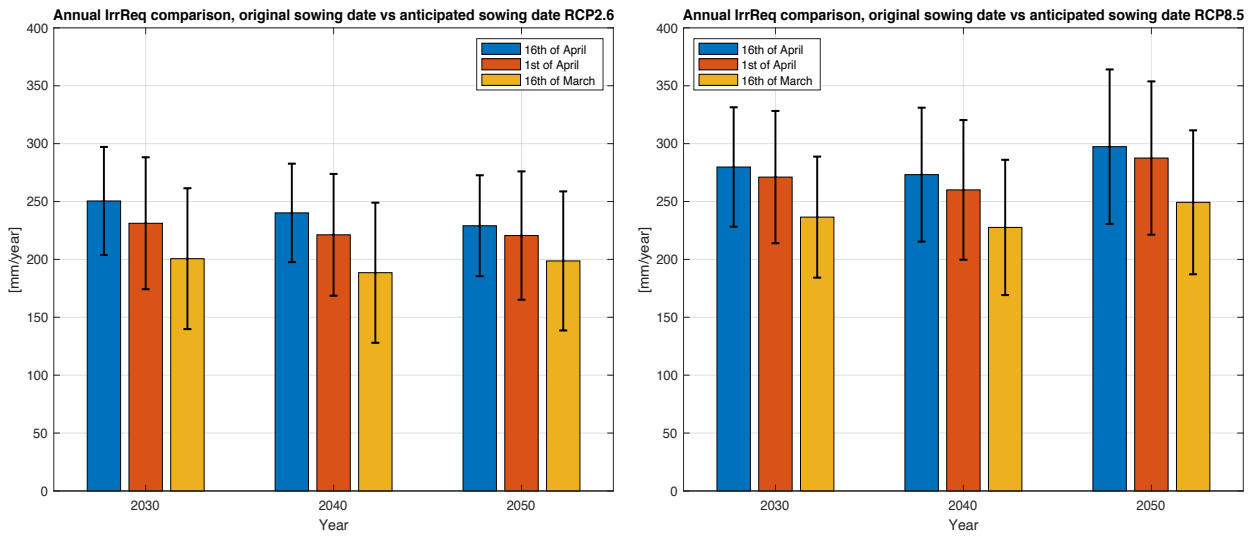


Figure 4.15: Comparison of annual *IrrReq* between the three different planting dates for the three future periods 2025-2034 (2030), 2035-2044 (2040), 2045-2054 (2050). Average upon the decades and standard deviation bars. 16th of April is the original planting date.

As demonstrated by the annual irrigation requirements comparison in Figure 4.15 and the values reported in Table 4.8, anticipating the sowing of maize seems always a good idea. The total annual *IrrReq* of maize planted in the two anticipated sowing dates are indeed always lower than the requirements of the original case, for both the climate scenarios, with peaks of decrement over -20% in some cases. The same consideration stands looking at the number of irrigation days shown in Table 4.9. Anticipating the sowing date of one month (March 16th) reduces the ID of percentages that in most cases exceed 10% (and even reach the 20% of decrement).

4.4 Crop adaptation, alternative crops

Another adaptation strategy is to change the crop to one less sensitive to water stress and less water demanding. In order to suggest alternative crops, the focus of these adaptation experiments was to find crops that are grown in spring/summer and check if they would require less irrigation water than maize.

In the area considered for this study, maize is the main cereal cultivated and also the main irrigated crop (ISTAT, 2010). After maize, the other two cereals more common over the Cuneo district are barley and wheat (Regione Piemonte, 2022). These two crops are usually cultivated from autumn to spring, so they are often not irrigated because during their development stages there is enough water available thanks to the more frequent winter/spring precipitations. Barley was not chosen, since its main season of growth is during winter and spring, so it is not a direct alternative for maize. Meanwhile, wheat is sometimes planted in spring too (and it is also more common in terms of hectares than barley, so more relevant in terms of production), so it was chosen as the first possible alternative crop to analyze. Wheat is a crop similar to maize and already common in the area, so it could be relatively easy for the farmers to implement this adaptation strategy if it is demonstrated to be useful. The second crop chosen was potato. Potato crop is not common in the area at the moment (ISTAT, 2010), but it was studied anyway because it is already present in the area even if in small percentage, and most importantly it has a very similar growing season to maize. It could be interesting to see if an increase in the hectares cultivated with potatoes could be beneficial in the changing climate conditions.

In this case, to perform the analyses it was required to substitute the inputs of the model about the crop type and the sowing-harvesting dates. No other inputs were changed to perform these new models runs. Table 4.10 reports the sowing and harvesting dates given as inputs to the model for wheat and potato, obtained from the MIRCA2000 database (Portmann et al., 2010).

Table 4.10: Sowing and Harvesting dates of maize, wheat and potato, between brackets there are the progressive number for the specific day in a year (from 0 to 365).

Experiment	Sowing	Harvesting
maize	16 th of April (106)	15 th of September (258)
wheat	16 th of April (106)	15 th of September (258)
potato	16 th of April (106)	15 th of October (288)

This experiment did not give the desired results, that is an alternative crop which will require less irrigation water than maize. As Figure 4.16 shows, neither wheat nor potato seem to be a better alternative to maize, requiring more water for irrigation in both the RCPs. Potato seems an especially bad alternative, and not a suitable crop in general in terms of irrigation requirements for the studied area of this work.

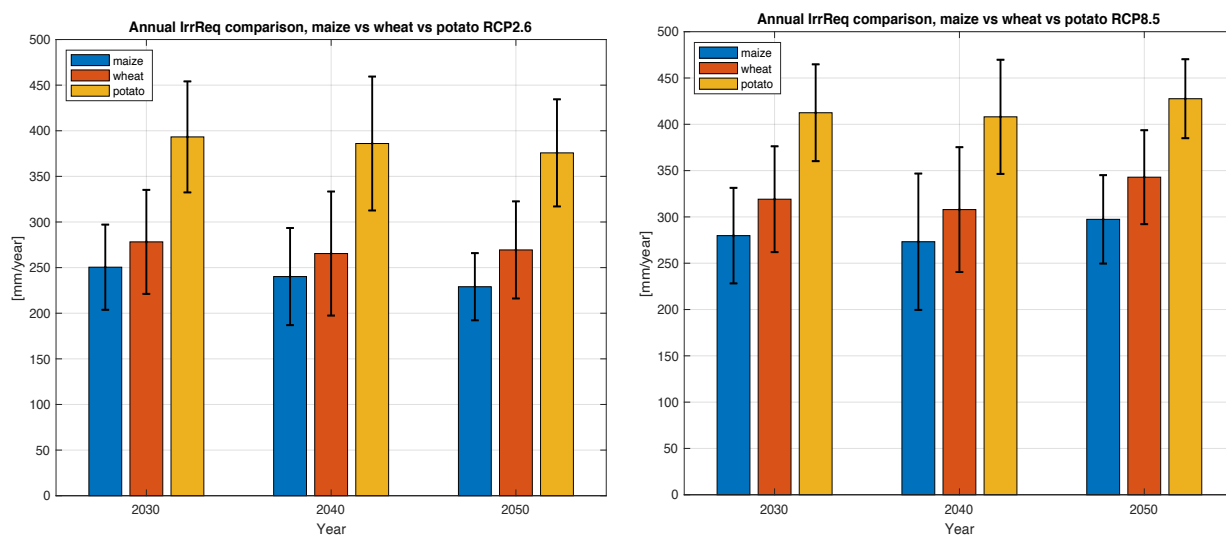


Figure 4.16: Comparison of annual irrigation requirements of maize, wheat, and potato for 2025-2034 (2030), 2035-2044 (2040), 2045-2054 (2050), both the climate scenarios RCP2.6 (left) and RCP8.5 (right). Average upon each decade and standard deviation bars.

Chapter 5 Conclusions

A local impact study was carried out in this work to evaluate the effects of climate change on the agriculture of a small area in the North-west of Italy, part of the district of Cuneo. In particular, the aim of the study was modelling the future evolution of maize's evapotranspiration and irrigation requirements in the area, with the hope of establishing a source of information for the implementation of effective adaptation plans.

The modelling was performed over the period 2006-2055 with a daily hydrological crop model already existing, which requires lots of information about both the crop investigated and the climate of the area. When modelling for the future period (2021-2055), we found that collecting the necessary data becomes more difficult, especially working at a smaller (local) scale. Great effort was then put into the preliminary phase of collecting data to obtain datasets as reliable as possible, with particular attention to the future climate projections. Datasets for precipitations and temperature under the two climate scenarios RCP2.6 and RCP8.5 were retrieved from five different combinations of GCMs (Global Climate Model) with RCMs (Regional Climate Model) to describe the range of climate change effects that can be expected.

In the area of interest for this work, maize is the most irrigated crop in terms of total hectares (ISTAT, 2010). The results confirmed that at the latitude of study, maize must be irrigated to maximize production, since in solely rainfed conditions the crop suffers from water stress for nearly 50% of its growing season (through all the period studied for both the RCPs). Furthermore, the most critical months in terms of water stress (and so in terms of precipitation water scarcity) turned out to be August and September. They are the only two months for which the number of severe water stress days (stress coefficient k_s less than 0.6) projected for the future from the two RCPs is more than zero.

Regarding irrigation requirements, it was demonstrated that this variable is sensitive to climate change, since there are visible differences between the projection under RCP2.6 and RCP8.5. RCP8.5 projects higher irrigation requirements for the future, with an average increase by 2050 of 16%. The projections under RCP2.6 were lower than RCP8.5 for all the climate datasets considered, with an average decrease of 13% in the irrigation requirements by 2050. The difference between the two scenarios is particularly evident over the last decade 2045-2054.

The number of irrigation days per year (days for which irrigation requirements are more than 2 mm/day) was computed as a useful index to clarify the situation. This index showed an increasing trend from 2006 to 2055 under RCP8.5 hypothesis, while it decreases under RCP2.6. It is important to note that while the high inter-annual variability of the results may limit the reliability of the trends indicated, the projections for RCP8.5 scenarios were nonetheless consistently higher than RCP2.6 projections.

The second part of the work consisted of assessing the efficiency of two possible adaptation strategies in reducing the future irrigation requirements of maize. The strategy of earlier sowing (and also earlier harvesting, to maintain a constant length of the growing season) could be an effective option to adapt to the projected climate changes in the area. Sowing before the original date (16th of April) by 15 days and by 31 days both resulted in a reduction of the future irrigation requirements, more evident in the case of the sowing on the 16th of March (31 days earlier). The positive effects are mainly due to the fact that earlier sowing allows earlier harvesting and so avoids the most critical period in terms of lack of precipitation and higher ET_0 (August and early September). The main advantage of this strategy is that it would be relatively easy for farmers to implement. The biggest disadvantage is the risk of late spring frosts happening after the sowing, which could negatively affect the production. It was not possible to study this aspect in this work, but it would be an interesting topic for further research. The second adaptation strategy considered was to substitute maize with less water demanding crops, so the aim of our modelling was to check if wheat and potato could be feasible options. We wanted options already cultivated in the area and as similar to maize in terms of agricultural techniques as possible, so that it would be relatively easy for farmers to eventually implement the strategy. Wheat and potato were the two crops that met these requirements. However, the results showed that they both required more irrigation than maize, especially potato. A suggestion for further studies then could be to analyze crops not yet present in the area but interesting in terms of climate resistance and market (i.e., economically attractive for the farmers) to find crops less sensitive to water stress than maize that could adapt better to the projected climate changes.

It is hoped that this thesis provides a relevant contribution to the knowledge about climate change impacts over the local area studied, with some useful data and considerations for the implementation of adaptation strategies. However, the work carried out demonstrated some of the difficulties of this type of local impact study. The main one is having to use crop models

which require lots of different input information, which is difficult to collect at the local scale, so a large amount of preliminary work of research and pre-processing of the information is needed in order to obtain reliable results.

References

- Allen R., Pereira L., Raes D., Smith E. M. (1998). Crop evapotranspiration: guidelines for computing crop water requirements FAO *irrigation and drainage paper 56* (Rome)
- ALPIMED (n.d). *PITER ALPIMED*. URL: <https://www.alpimed.eu/it/piter-alpimed-2/> [Accessed: September 2022]
- Arpa Piemonte (2010). *Metodologia Analisi NWIOI*
- Arpa Piemonte (2017). *NWIOI 2.1 dataset*. URL: <https://www.arpa.piemonte.it/rischinaturali/tematismi/clima/confronti-storici/dati/dati.html> [Accessed: May 2022]
- Arpa Piemonte, Regione Piemonte (2020°). *Analisi degli scenari di clima regionale del periodo 2011- 2100*
- Arpa Piemonte, Regione Piemonte (2020b). *Analisi del clima regionale del periodo 1981-2010 e tendenze negli ultimi 60 anni*
- Baldauf, M., Seifert, A., Förstner, J., Majewski, D., Raschendorfer, M., Reinhardt, T., Baldauf, M., Seifert, A., Förstner, J., Majewski, D., Raschendorfer, M., and Reinhardt, T. (2011). *Operational Convective-Scale Numerical Weather Prediction with the COSMO Model: Description and Sensitivities*, Mon. Weather Rev., 139, 3887–3905, <https://doi.org/10.1175/MWR-D-10-05013.1>
- Bentsen, M., Bethke, I., Debernard, J. B., Iversen, T., Kirkevåg, A., Seland, Ø., Drange, H., Roelandt, C., Seierstad, I. A., Hoose, C., and Kristjánsson, J. E. (2013). *The Norwegian Earth System Model, NorESM1-M – Part 1: Description and basic evaluation of the physical climate*, Geosci. Model Dev., 6, 687–720, <https://doi.org/10.5194/gmd-6-687-2013>.
- Cappellini M. (2022). *La siccità abbatte il Pil agricolo del 10%. Danni alle imprese per 6 miliardi di euro*. URL: <https://www.ilsole24ore.com/art/la-siccita-abbatte-pil-agricolo-10percento-danni-impres-6-miliardi-euro-AE8Yc5nB>
- C3S (Copernicus Climate Change Service), (2022a). *Evaluation of CDS climate projections*. URL: <https://confluence.ecmwf.int/display/CKB/Evaluation+of+CDS+climate+projections> [Accessed: August 2022]
- C3S (Copernicus Climate Change Service), (2022b). *CORDEX: Regional climate projections, List of published parameters*. URL: <https://confluence.ecmwf.int/display/CKB/CORDEX%3A+Regional+climate+projections#CORDEX:Regionalclimateprojections-Listofpublishedparameters> [Accessed: August 2022]

- CDS (Climate Data Store), (2022). *CORDEX regional climate model data on single levels*. DOI: 10.24381/cds.bc91edc3. URL: <https://cds.climate.copernicus.eu/cdsapp#!/dataset/projections-cordex-domains-single-levels?tab=overview> [Accessed: April 2022]
- IlPuntoColdiretti (2022). *Siccità: 250mila aziende agricole a rischio crack, ecco la mappa dei danni*. URL: <https://www.ilpuncocoldiretti.it/attualita/economia/siccita-250mila-aziende-agricole-a-rischio-crack-ecco-la-mappa-dei-danni/> [Accessed: August 2022]
- Eaton B., Gregory J., Drach B., Taylor K., Hankin S., Blower J., Caron J., Signell R., Bentley P., Rappa G., Höck H., Pamment A., Juckes M., Raspaud M., Horne R., Whiteaker T., Blodgett D., Zender C., Lee D., Hassell D., Snow A. D., Kölling T., Allured D., Jelenak A., Soerensen A. M., Gaultier L., Herlédan S. (2021). *NetCDF Climate and Forecast (CF) Metadata Conventions*.
- EURO-CORDEX community (2021). *Guidance for EURO-CORDEX climate projections data use*
- FAO (2021a). *GAEZ, Global Agro-Ecological Zones*. URL: <https://gaez.fao.org> [Accessed: May 2022]
- FAO (2021b). *The State of the World's Land and Water Resources for Food and Agriculture – Systems at breaking point. Synthesis report 2021*. Rome. <https://doi.org/10.4060/cb7654en>
- G. H. Fang, J. Yang, Y. N. Chen, and C. Zammit (2015) *Comparing bias correction methods in downscaling meteorological variables for a hydrologic impact study in an arid area in China*, Hydrol. Earth Syst. Sci., 19, 2547–2559
- Giorgetta, M. A., Jungclaus, J., Reick, C. H., Legutke, S., Bader, J., Böttinger, M., Brovkin, V., Crueger, T., Esch, M., Fieg, K., Glushak, K., Gayler, V., Haak, H., Hollweg, H.-D., Ilyina, T., Kinne, S., Kornbluh, L., Matei, D., Mauritsen, T., Mikolajewicz, U., Mueller, W., Notz, D., Pithan, F., Raddatz, T., Rast, S., Redler, R., Roeckner, E., Schmidt, H., Schnur, R., Segschneider, J., Six, K. D., Stockhause, M., Timmreck, C., Wegner, J., Widmann, H., Wieners, K.-H., Claussen, M., Marotzke, J., and Stevens, B., (2013). *Climate and carbon cycle changes from 1850 to 2100 in MPI-ESM simulations for the Coupled Model Intercomparison Project phase 5*, J. Adv. Model. Earth Sy., 5, 572–597, <https://doi.org/10.1002/jame.20038>
- Google, n.d. [Google Map of the area near Cuneo, Italy, modified using Google MyMaps]. Retrieved September 30th 2022.
- Hargreaves GH, Samani ZA. (1985). *Reference Crop Evapotranspiration from Temperature*. Applied Engineering in Agriculture: p. 96–99
- Hazeleger, W., Severijns, C., Semmler, T., Ștefănescu, S., Yang, S., Wang, X., Wyser, K., Dutra, E., Baldasano, J. M., Bintanja, R., Bougeault, P., Caballero, R., Ekman, A. M. L., Christensen, J. H., van den Hurk, B., Jimenez, P., Jones, C., Källberg, P., Koenig, T., McGrath, R., Miranda, P., van Noije, T., Palmer, T., Parodi, J. A., Schmith, T., Selten, F., Storelvmo, T., Sterl, A., Tapamo, H., Vancoppenolle, M., Viterbo, P., &

Willén, U., (2010). *EC-Earth*, *Bulletin of the American Meteorological Society*, 91(10), 1357-1364, <https://doi.org/10.1175/2010BAMS2877.1>

IPCC (2021). *Summary for Policymakers. In: Climate Change 2021: The Physical Science Basis. Contribution of Working Group I to the Sixth Assessment Report of the Intergovernmental Panel on Climate Change [Masson-Delmotte, V., P. Zhai, A. Pirani, S.L. Connors, C. P'ean, S. Berger, N. Caud, Y. Chen, L. Goldfarb, M.I. Gomis, M. Huang, K. Leitzell, E. Lonnoy, J.B.R. Matthews, T.K. Maycock, T. Waterfield, O. Yelekci, R. Yu, and B. Zhou (eds.)]*. In Press, 2021.

ISTAT (2010). *6° censimento agricoltura 2010*. URL: <http://dati-censimentoagricoltura.istat.it/Index.aspx> [Accessed: April 2022]

Iturbide, M., Gutiérrez, J. M., Alves, L. M., Bedia, J., Cerezo-Mota, R., Gimadevilla, E., Cofiño, A. S., Di Luca, A., Faria, S. H., Gorodetskaya, I. V., Hauser, M., Herrera, S., Hennessy, K., Hewitt, H. T., Jones, R. G., Krakovska, S., Manzanaras, R., Martínez-Castro, D., Narisma, G. T., Nurhati, I. S., Pinto, I., Seneviratne, S. I., van den Hurk, B., and Vera, C. S. (2020). *An update of IPCC climate reference regions for subcontinental analysis of climate model data: definition and aggregated datasets*, *Earth Syst. Sci. Data*, 12, 2959–2970, <https://doi.org/10.5194/essd-12-2959-2020>

Jacob, D.; Petersen, J.; Eggert, B.; Alias, A.; Christensen, O. B.; Bouwer, L. M.; Braun, A.; Colette, A.; Déqué, M.; Georgievski, G.; Georgopoulou, E.; Gobiet, A.; Menut, L.; Nikulin, G.; Haensler, A.; Hempelmann, N.; Jones, C.; Keuler, K.; Kovats, S.; Kröner, N.; Kotlarski, S.; Kriegsmann, A.; Martin, E.; van Meijgaard, E.; Moseley, C.; Pfeifer, S.; Preuschmann, S.; Radermacher, C.; Radtke, K.; Rechid, D.; Rounsevell, M.; Samuelsson, P.; Somot, S.; Soussana, J.-F.; Teichmann, C.; Valentini, R.; Vautard, R.; Weber, B. & Yiou, P. (2014). *EURO-CORDEX: new high-resolution climate change projections for European impact research Regional Environmental Changes*. Vol. 14, Issue 2, pp. 563-578., <https://doi.org/10.1007/s10113-013-0499-2>

Kreienkamp F., Huebener H., Linke C., and Spekat A. (2012). *Good practice for the usage of climate model simulation results - a discussion paper*, *Environmental Systems Research* 1:9, doi:10.1186/2193-2697-1-9

Mbow, C., C. Rosenzweig, L. G. Barioni, T. G. Benton, M. Herrero, M. Krishnapillai, E. Liwenga, P. Pradhan, M. G. Rivera-Ferre, T. Sapkota, F. N. Tubiello, Y. Xu (2019). *Food Security. In: Climate Change and Land: an IPCC special report on climate change, desertification, land degradation, sustainable land management, food security, and greenhouse gas fluxes in terrestrial ecosystems [P.R. Shukla, J. Skea, E. Calvo Buendia, V. Masson-Delmotte, H.-O. Pörtner, D.C. Roberts, P. Zhai, R. Slade, S. Connors, R. van Diemen, M. Ferrat, E. Haughey, S. Luz, S. Neogi, M. Pathak, J. Petzold, J. Portugal Pereira, P. Vyas, E. Huntley, K. Kissick, M. Belkacemi, J. Malley, (eds.)]*. In press.

Portmann F, Siebert S., and Döll E. P. (2010). *MIRCA2000—Global monthly irrigated and rainfed crop areas around the year 2000: a new high-resolution data set for agricultural and hydrological modeling* *Glob. Biogeochem. Cycles* 24 GB1011

- Regione Piemonte (n.d). *La rete irrigua e i canali del Piemonte*. URL: <https://www.regione.piemonte.it/web/temi/agricoltura/agroambiente-meteo-suoli/rete-irrigua-canali-piemonte> [Accessed: May 2022]
- Regione Piemonte (2022). *Anagrafe agricola - data warehouse*. URL: <https://servizi.regione.piemonte.it/catalogo/anagrafe-agricola-data-warehouse> [Accessed: July 2022]
- Rolle M., Tamea S., Claps P. (2021). *ERA5- based global assessment of irrigation requirement and validation*. PLoS ONE 16(4): e0250979. <https://doi.org/10.1371/journal.pone.0250979>
- Rolle M., Tamea S., Claps P. (2022). *Climate-driven trends in agricultural water requirement: an ERA5-based assessment at daily scale over 50 years*, Environ. Res. Lett. 17 044017
- Rosenzweig C., Elliott J., Deryng D., Ruane A. C., Müller C., Arneth A., Boote K. J., Folberth C., Glotter M., Khabarov N., Neumann K., Piontek F., Pugh T. A. M., Schmid E., Stehfest E., Yang H., and Jones J. W., (2014). *Assessing agricultural risks of climate change in the 21st century in a global gridded crop model intercomparison*. Proceedings of the National Academy of Sciences 111, 9 (2014), 3268–3273
- Bassu S., Fumagalli D., Toreti A., Ceglar A., Giunta F., Motzo F., Zajac Z., Niemeyer S., (2021). *Modelling potential maize yield with climate and crop conditions around flowering*
- Strandberg, G., Barring, L., Hansson, U., Jansson, C., Jones, C., Kjellström, E., Kolax, M., Kupiainen, M., Nikulin, G., Samuelsson, P., Ullerstig, A., and Wang, S., (2014). *CORDEX scenarios for Europe from the Rossby Centre regional climate model RCA4*, Report meteorology and climatology No. 116, Swedish Meteorological and Hydrological Institute (SMHI), ISSN: 0347-2116.
- Tuninetti M, Tamea S, D’Odorico P, Laio F and Ridolfi E L (2015). *Global sensitivity of high-resolution estimates of crop water footprint* Water Resour. Res. 51 8257–72
- Campbell R. (2022). *Shaded Error Bar*, GitHub. URL: <https://github.com/raacampbell/shadedErrorBar> Retrieved September 25th, 2022.
- van Meijgaard, E., van Ulf, B., van de Berg, W. J., Bosveld, F. C., van den Hurk, B., Lenderink, G., and Siebesma, A. P., (2008). *The KNMI regional atmospheric climate model RACMO version 2.1 (KNMI TR-302)*, Tech. Rep., Technical Report TR-302.
- WCRP (2022). *Coordinated Regional Climate Downscaling Experiment - About*. URL: <https://cordex.org/about/> [Accessed: August 2022]

Appendix I – Climate projections databases

Table I.1: Results of the research for climate future projections datasets available on the internet at the time of this study

Dataset	Domain	horizontal resolution	temporal coverage	Temperature	Precipitations	Climate scenarios
CORDEX regional climate model data on single levels [1]	Europe	0.11°x0.11° 0.44°x0.44°	2006-2100	Daily average, max, min temperature (K)	Daily precipitations (kg/m ² s)	RCPs (2.6,4.5,8.5)
Soil erosion indicators for Italy from 1981 to 2080 [2]	Italy	0.11°x0.11°	1981-2080	-	Total precipitations (kg m ⁻²)	Current, RCPs (2.6,4.5,8.5)
Climate, energy indicators Europe 2005-2100 from climate projections [3]	Europe	0.25° x 0.25°	2005-2100	Temperature (K)	Total precipitations (m)	RCPs (2.6,4.5,8.5)
Temperature statistics for Europe from climate projections [4]	Europe	0.1° x 0.1°	1986-2085	Average, max and min temperature (K)	-	RCP4.5 and RCP8.5
Temperature and precipitation CII's 1970-2100 from European climate projections [5]	Europe	0.11°x0.11° 5kmx5km	1970-2100	Temperature (°C)	Precipitations (mm/day)	Temperature increase of 1.5, 2.0 and 3.0 °C
CMIP6 climate projections [6]	Global	varies between models	2015-2100	Temperature (K)	Precipitations (kg m ⁻² s ⁻¹)	SSP5-8.5, SSP3-7.0, SSP2-4.5, SSP1-2.6, SSP4-6.0, SSP4-3.4, SSP5-3.4OS, SSP1-1.9
NASA Earth Exchange (NEX) Downscaled Climate Projections (NEX-DCP30) [7]	CONUS (USA)	30x30 arc second	2006-2099	Monthly averaged max and min temperature (K)	Daily precipitation rate (kg m ⁻² s ⁻¹)	RCPs (2.6,4.5,8.5)

North American Regional Climate Change Assessment Program (NARCCAP) [8]	USA and most of Canada	50kmx50km	1971-2000 2041-2070	min and max daily temperature,	precipitation (3 hours)	A2 emissions scenario (SRES)
--	------------------------	-----------	------------------------	--------------------------------	-------------------------	------------------------------

Note for datasets references:

- [1] CDS (Climate Data Store). *CORDEX regional climate model data on single levels*. DOI: 10.24381/cds.bc91edc3. URL: <https://cds.climate.copernicus.eu/cdsapp#!/dataset/projections-cordex-domains-single-levels?tab=overview> [Accessed: April 2022]
- [2] Santini M., Rianna G., Mancini M., Stojiljkovic M., Padulano R., Noce S. (2021): Soil erosion indicators for Italy from 1981 to 2080, version 1.0, Copernicus Climate Change Service (C3S) Climate Data Store (CDS), 10.24381/cds.66d88ff8
- [3] CDS (Climate Data Store). *Climate and energy indicators for Europe from 2005 to 2100 derived from climate projections*. DOI: <https://doi.org/10.24381/cds.f6951a62> URL: <https://cds.climate.copernicus.eu/cdsapp#!/dataset/sis-energy-derived-projections?tab=overview>
- [4] CDS (Climate Data Store). *Temperature statistics for Europe derived from climate projections*. DOI: <https://doi.org/10.24381/cds.8be2c014> URL: <https://cds.climate.copernicus.eu/cdsapp#!/dataset/sis-temperature-statistics?tab=overview>
- [5] Berg, P, Photiadou, C, Simonsson, L, Sjökvist, E, Thuresson, J, and Mook, R, (2021): *Temperature and precipitation climate impact indicators from 1970 to 2100 derived from European climate projections*, version 1, Copernicus Climate Change Service (C3S) Climate Data Store (CDS), DOI: 10.24381/cds.9eed87d5
- [6] CDS (Climate Data Store). *CMIP6 climate projections*. DOI: <https://doi.org/10.24381/cds.c866074c> URL: <https://cds.climate.copernicus.eu/cdsapp#!/dataset/projections-cmip6?tab=overview>
- [7] NCCS, NASA Center for Climate Simulation. *NASA Earth Exchange (NEX) Downscaled Climate Projections (NEX-DCP30)*. URL: <https://www.nccs.nasa.gov/services/data-collections/land-based-products/nex-dcp30>
- [8] NARCCAP, North American Regional Climate Change Assessment Program. URL: <http://www.narccap.ucar.edu/data/status.html>

Appendix II – Validation graphs for T_{max} and T_{min}

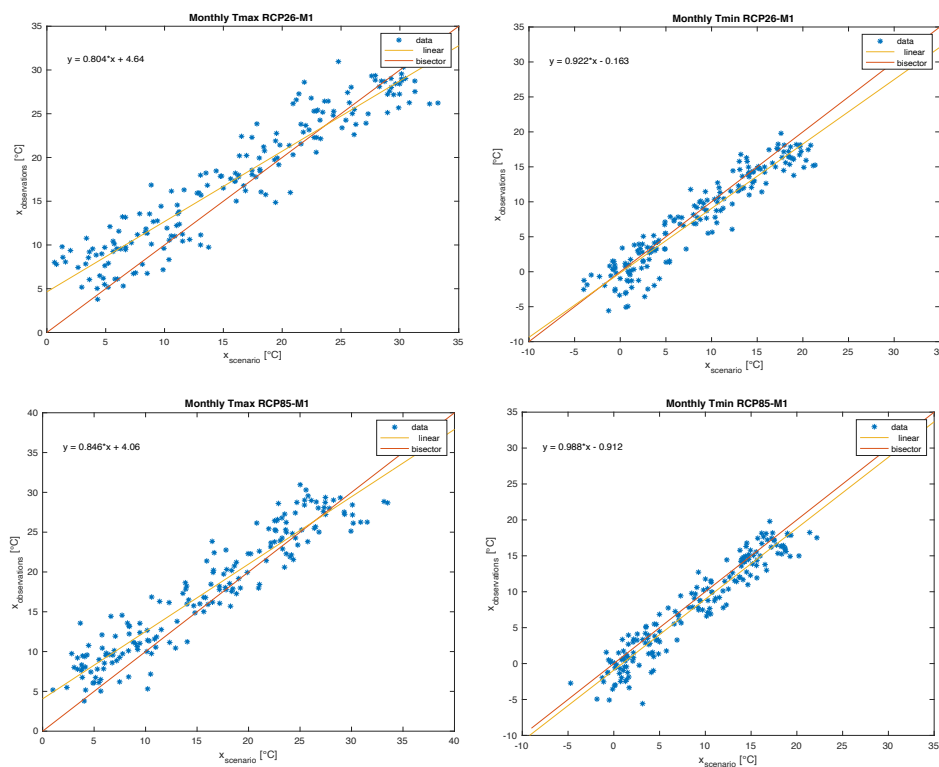


Figure II.1: Validation graphs for RCP26-M1 (top) and RCP85-M1 (bottom), both T_{max} (left) and T_{min} (right). The line of the linear fitting and its equation, as well as the bisector of the quadrant are shown.

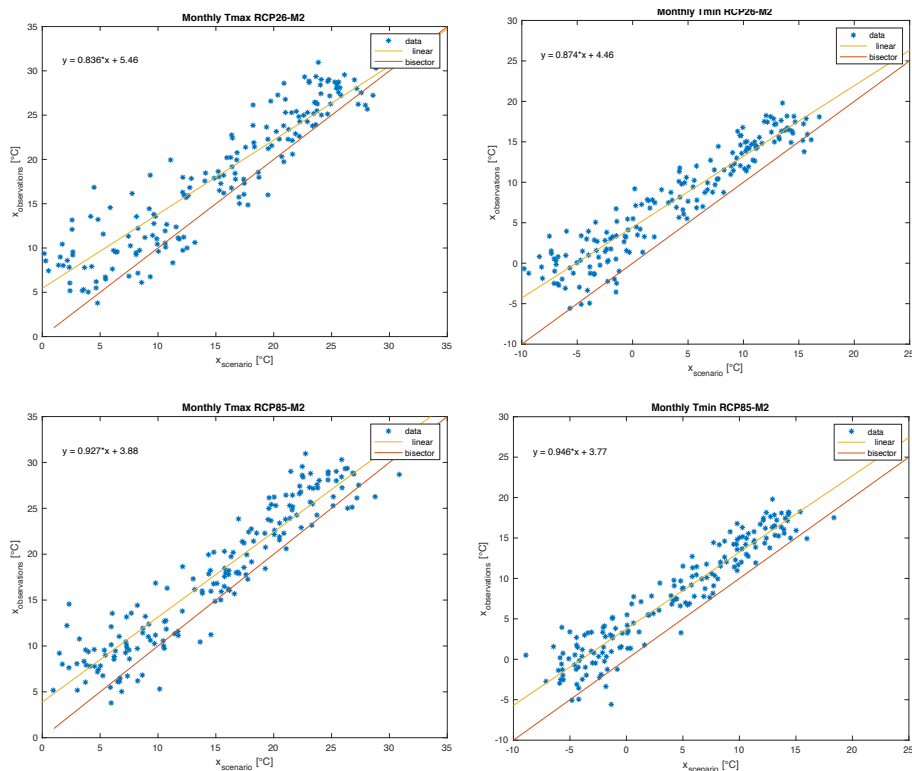


Figure II.2: Validation graphs for RCP26-M2 (top) and RCP85-M2 (bottom), both T_{max} (left) and T_{min} (right). The line of the linear fitting and its equation, as well as the bisector of the quadrant are shown.

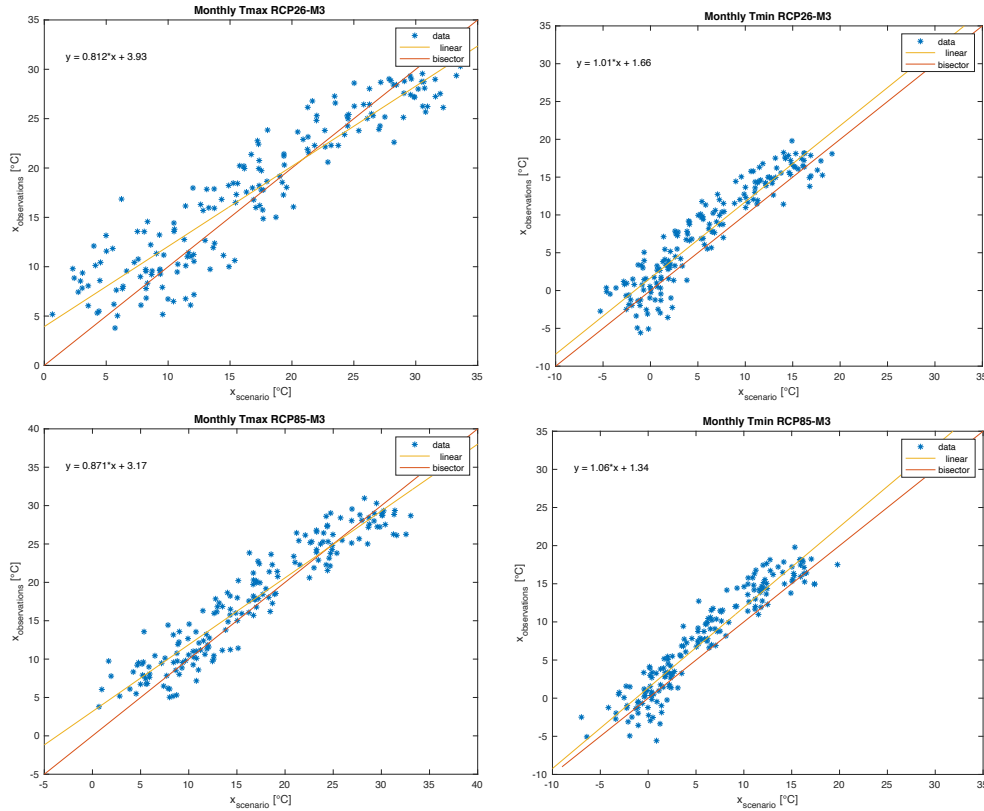


Figure II.3: Validation graphs for RCP26-M3 (top) and RCP85-M3 (bottom), both T_{max} (left) and T_{min} (right). The line of the linear fitting and its equation, as well as the bisector of the quadrant are shown.

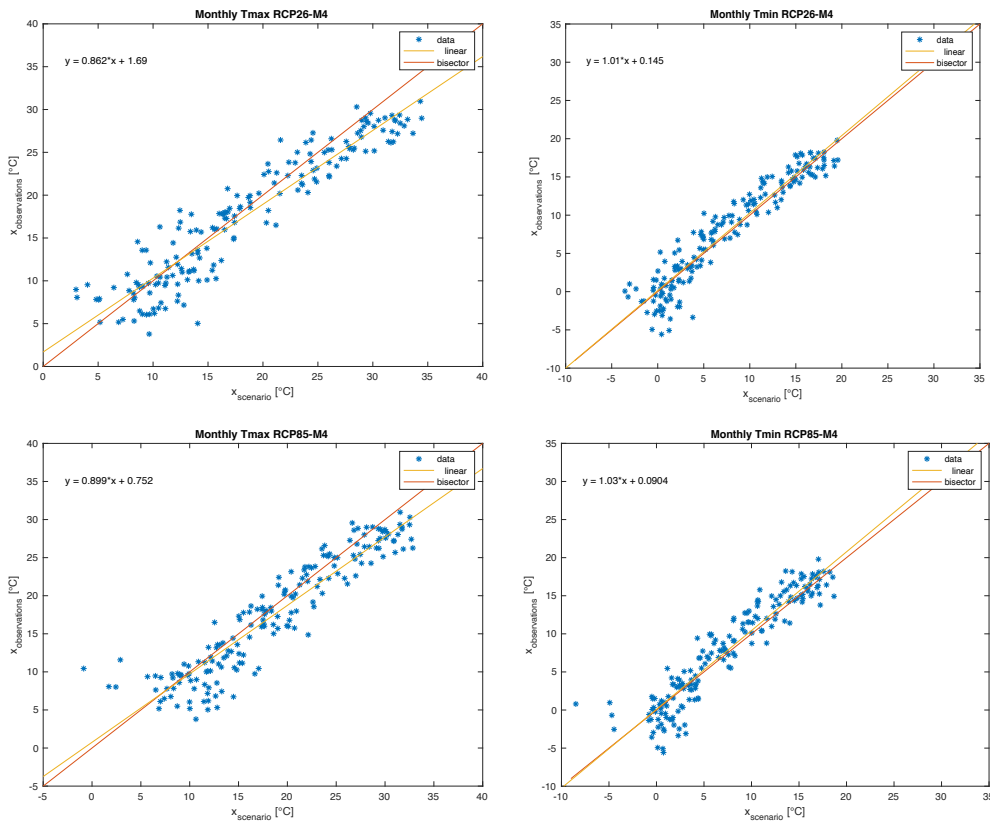


Figure II.4: Validation graphs for RCP26-M4 (top) and RCP85-M4 (bottom), both T_{max} (left) and T_{min} (right). The line of the linear fitting and its equation, as well as the bisector of the quadrant are shown.

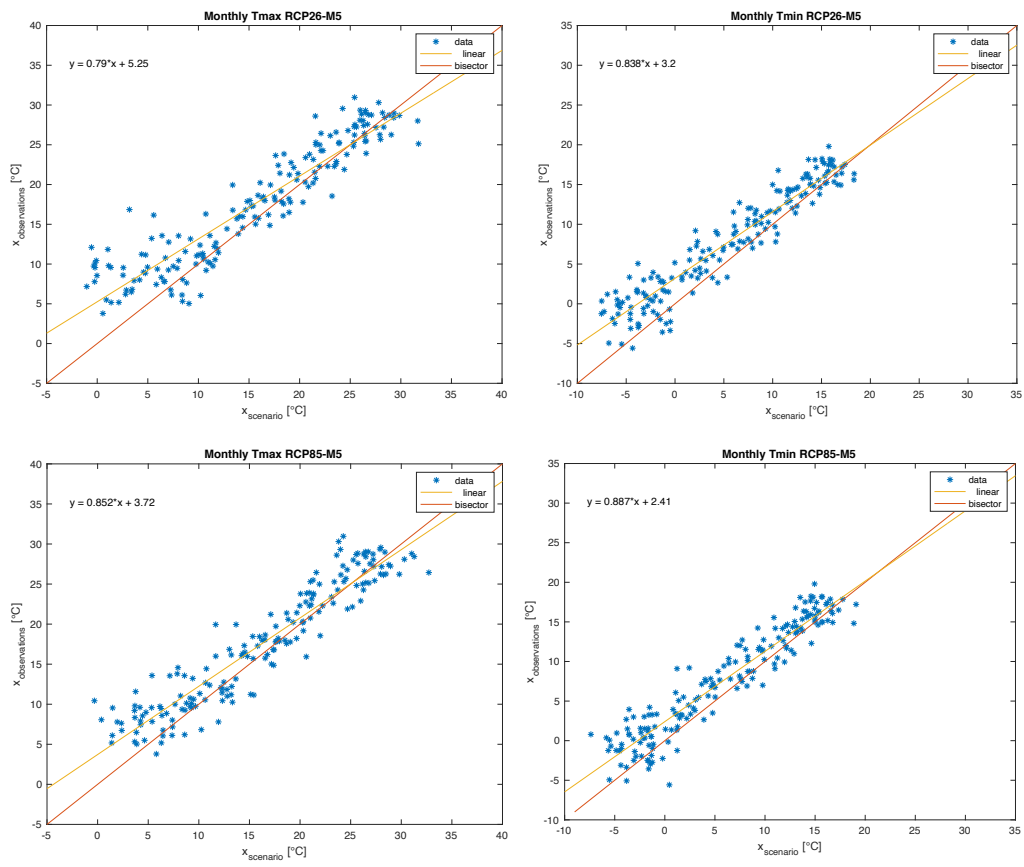


Figure II.5: Validation graphs for RCP26-M5 (top) and RCP85-M5 (bottom), both T_{\max} (left) and T_{\min} (right). The line of the linear fitting and its equation, as well as the bisector of the quadrant are shown.

Appendix III – Validation graphs for precipitations

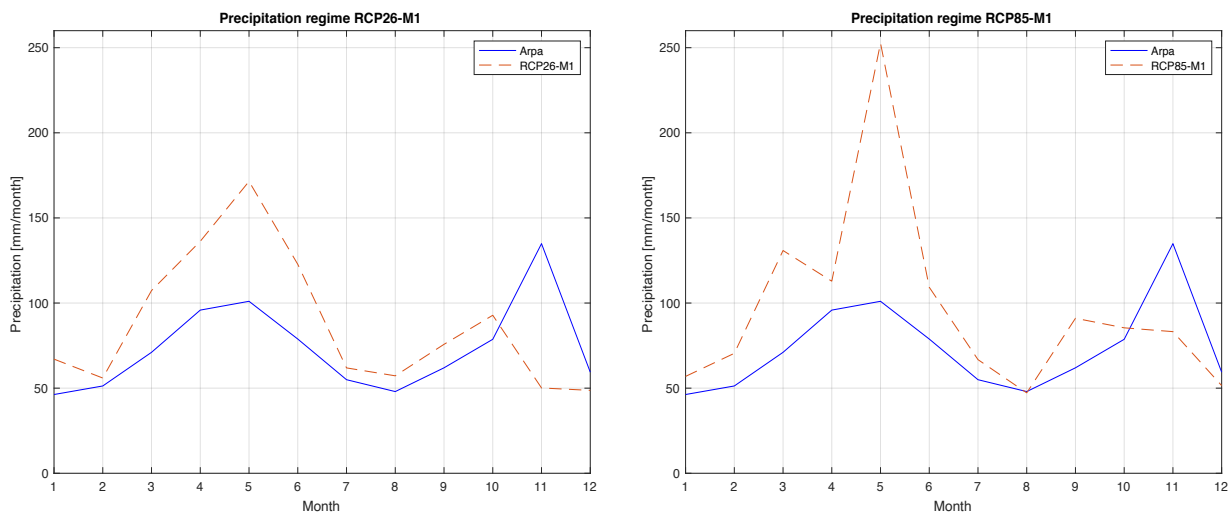


Figure III.1: Comparison between the precipitation regime (average monthly precipitation) of RCP26-M1 (left) and RCP85-M1 (right) and the regime showcased by the Arpa Piemonte observations (Arpa Piemonte, 2017) from 2006 to 2020.

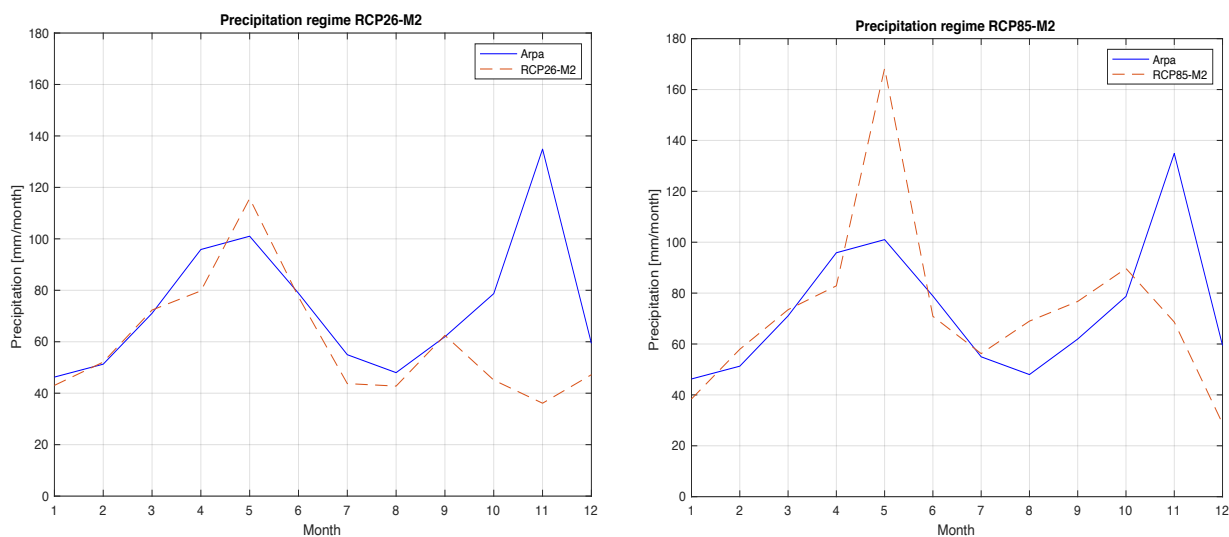


Figure III.2: Comparison between the precipitation regime (average monthly precipitation) of RCP26-M2 (left) and RCP85-M2 (right) and the regime showcased by the Arpa Piemonte observations (Arpa Piemonte, 2017) from 2006 to 2020.

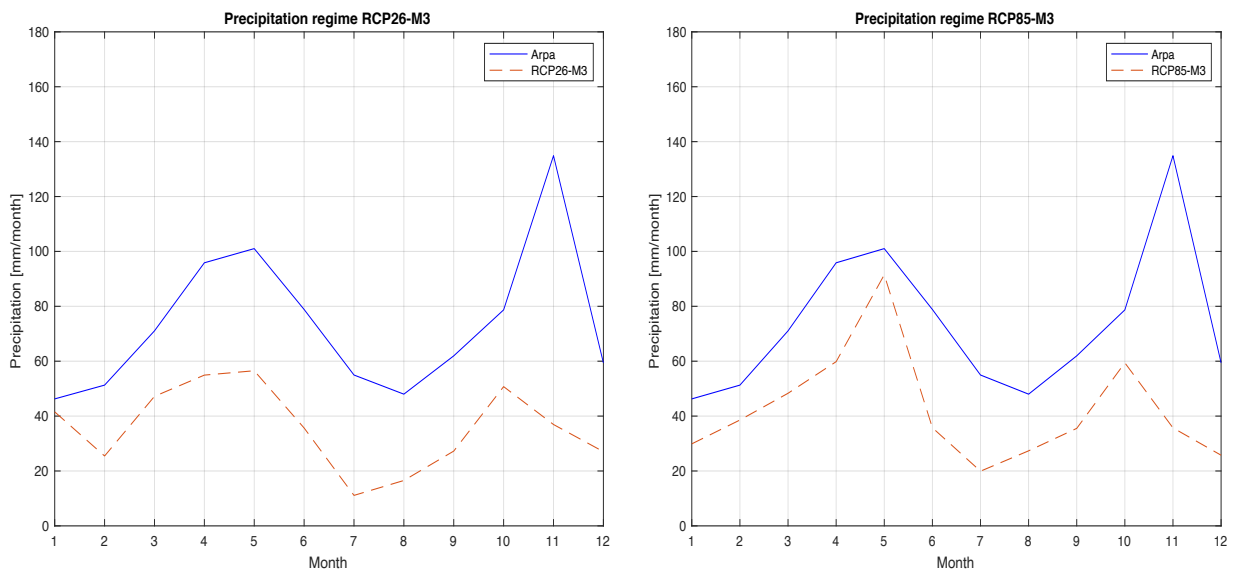


Figure III.3: Comparison between the precipitation regime (average monthly precipitation) of RCP26-M3 (left) and RCP85-M3 (right) and the regime showcased by the Arpa Piemonte observations (Arpa Piemonte, 2017) from 2006 to 2020.

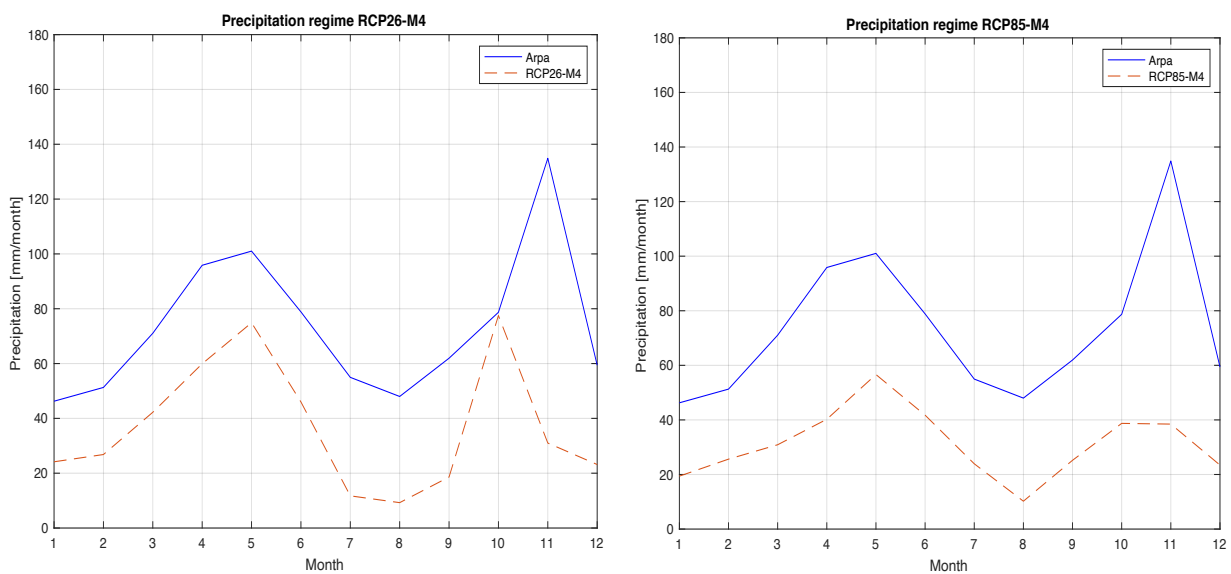


Figure III.4: Comparison between the precipitation regime (average monthly precipitation) of RCP26-M4 (left) and RCP85-M4 (right) and the regime showcased by the Arpa Piemonte observations (Arpa Piemonte, 2017) from 2006 to 2020.

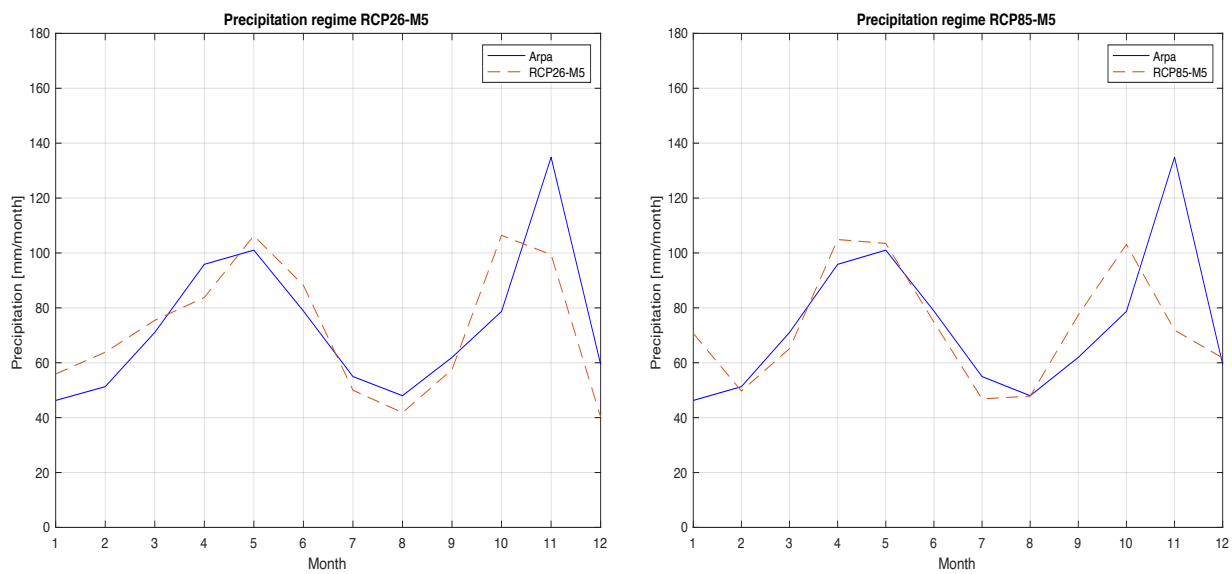


Figure III.5: Comparison between the precipitation regime (average monthly precipitation) of RCP26-M5 (left) and RCP85-M5 (right) and the regime showcased by the Arpa Piemonte observations (Arpa Piemonte, 2017) from 2006 to 2020.

Acknowledgments

I would like to express my gratitude to my thesis supervisor, Prof. Stefania Tamea, for the opportunity of working on this challenging but interesting topic, and for the support through these months of work.

I would also like to thank Dr. Matteo Rolle for providing me the needed materials for the analyses, and for the useful insights on the subject.

Finally, I wish to extend my appreciation to all my friends and family, with a special thanks to my mother whose endless support has been of immeasurable value.